TECH BRIEFS

NATIONAL AERONAUTICS AND SPACE ADMINISTRATION

INTRODUCTION

Tech Briefs are short announcements of innovations originating from research and development activities of the National Aeronautics and Space Administration. They emphasize information considered likely to be transferable across industrial, regional, or disciplinary lines and are issued to encourage commercial application.

Availability of NASA Tech Briefs and TSPs

Requests for individual Tech Briefs or for Technical Support Packages (TSPs) announced herein should be addressed to

National Technology Transfer Center

Telephone No. **(800) 678-6882** or via World Wide Web at **www2.nttc.edu/leads/**

Please reference the control numbers appearing at the end of each Tech Brief. Information on NASA's Innovative Partnerships Program (IPP), its documents, and services is also available at the same facility or on the World Wide Web at **http://ipp.nasa.gov**.

Innovative Partnerships Offices are located at NASA field centers to provide technology-transfer access to industrial users. Inquiries can be made by contacting NASA field centers listed below.

NASA Field Centers and Program Offices

Ames Research Center
Lisa L. Lockyer
(650) 604-1754
lisa.l.lockyer@nasa.gov

Dryden Flight Research Center
Gregory Poteat
(661) 276-3872
greg.poteat@dfrc.nasa.gov

Goddard Space Flight Center
Nona Cheeks
(301) 286-5810
nona.k.cheeks@nasa.gov

Jet Propulsion Laboratory
Ken Wolfenbarger
(818) 354-3821
james.k.wolfenbarger@jpl.nasa.gov

Johnson Space Center
Michele Brekke
(281) 483-4614
michele.a.brekke@nasa.gov

Kennedy Space Center
David R. Makufka
(321) 867-6227
david.r.makufka@nasa.gov

Langley Research Center
Martin Waszak
(757) 864-4052
martin.r.waszak@nasa.gov

Glenn Research Center
Robert Lawrence
(216) 433-2921
robert.f.lawrence@nasa.gov

Marshall Space Flight Center
Vernotto McMillan
(256) 544-2615
vernotto.mcmillan@msfc.nasa.gov

Stennis Space Center
John Bailey
(228) 688-1660
john.w.bailey@nasa.gov

Carl Ray, Program Executive
Small Business Innovation
Research (SBIR) & Small
Business Technology
Transfer (STTR) Programs
(202) 358-4652
carl.g.ray@nasa.gov

Merle McKenzie
Innovative Partnerships
Program Office
(202) 358-2560
merle.mckenzie-1@nasa.gov

NASA Tech Briefs

NATIONAL AERONAUTICS AND SPACE ADMINISTRATION

Technology Focus:
Test & Measurement

✱ Simulator for Testing Spacecraft Separation Devices

Marshall Space Flight Center, Alabama

A report describes the main features of a system for testing pyrotechnic and mechanical devices used to separate spacecraft and modules of spacecraft during flight. The system includes a spacecraft simulator [also denoted a large mobility base (LMB)] equipped with air thrusters, sensors, and data-acquisition equipment. The spacecraft simulator floats on air bearings over an epoxy-covered concrete floor. This free-flotation arrangement enables simulation of motion in outer space in three degrees of freedom: translation along two orthogonal horizontal axes and rotation about a vertical axis. The system also includes a static stand. In one application, the system was used to test a bolt-retraction system (BRS) intended for separation of the lifting-body and deorbit-propulsion stages of the X-38 spacecraft. The LMB was connected via the BRS to the static stand, then pyrotechnic devices that actuate the BRS were fired. The separation distance and acceleration were measured. The report cites a document, not yet published at the time of reporting the information for this article, that is said to present additional detailed information.

This work was done by Nick Johnston, Joe Gaines, and Tom Bryan of **Marshall Space Flight Center**. *For further information, contact Sammy Nabors, MSFC Commercialization Assistance Lead, at sammy.a.nabors@nasa.gov. Refer to MFS-31907.*

⊕ Apparatus for Hot Impact Testing of Material Specimens
It is not necessary to cool and reheat the furnace between tests.

John H. Glenn Research Center, Cleveland, Ohio

An apparatus for positioning and holding material specimens is a major subsystem of a system for impact testing of the specimens at temperatures up to 1,500 °C. This apparatus and the rest of the system are designed especially for hot impact testing of advanced ceramics, composites, and coating materials.

The apparatus includes a retaining fixture on a rotating stage on a vertically movable cross support driven by a linear actuator. These components are located below a furnace wherein the hot impact tests are performed (see Figure 1). In preparation for a test, a specimen is mounted on the retaining fixture, then the cross support is moved upward to raise the specimen, through an opening in the bottom of the
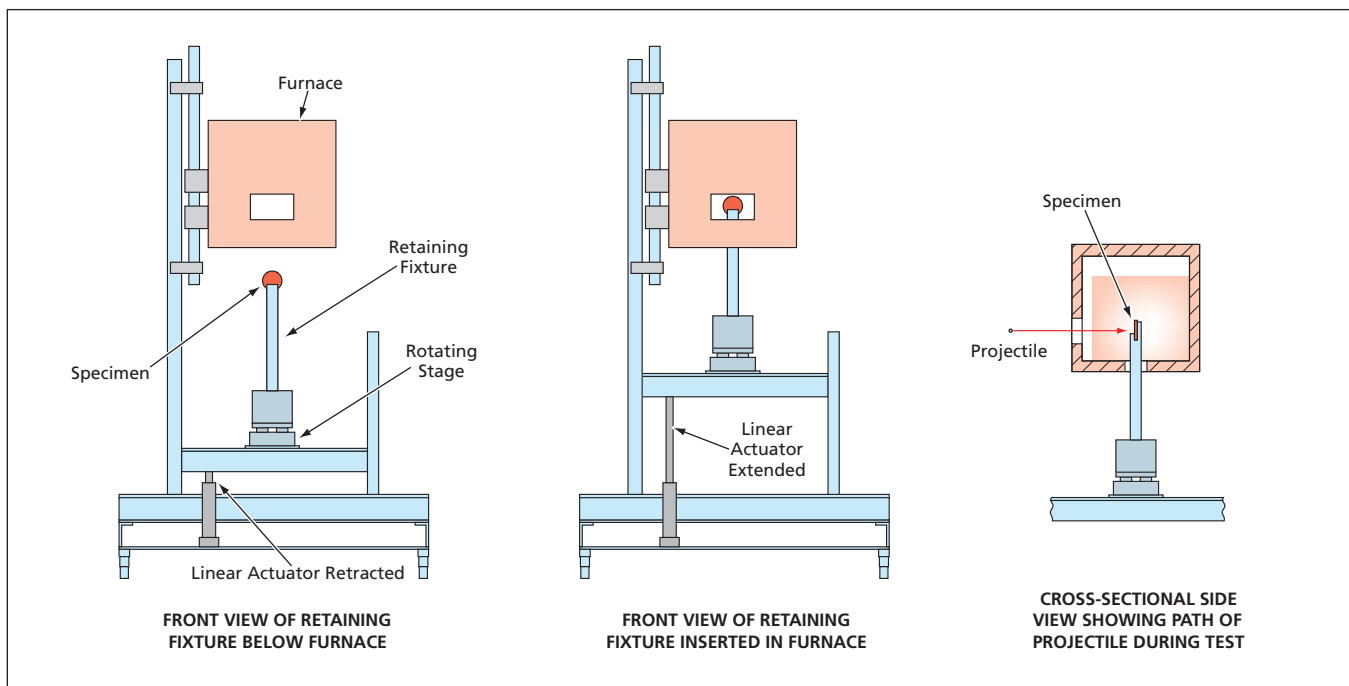

Figure 1. The **Retaining Fixture and Specimen** are raised into the furnace, wherein the specimen is heated and subjected to impact by a projectile.

furnace, to the test position inside the furnace. On one side of the furnace there is another, relatively small opening on a direct line to the specimen. Once the specimen has become heated to the test temperature, the test is performed by using an instrumented external pressurized-gas-driven gun to shoot a projectile through the side opening at the specimen.

Advantageous features of the design and operation of this apparatus include the following:

• All parts of the retaining fixture are made of silicon carbide to withstand high test temperatures.
• The simplest version of the retaining fixture (see Figure 2) includes a tube, into which are machined tapered slots to accommodate a flat specimen and a side hole for admitting a projectile. (In a more complex version, there are slots for two specimens and two corresponding projectile holes at diametrically opposite locations.) The specimen is held in place by silicon carbide wedges inserted in the tapered gaps remaining between the specimen and the slots.
• Among the alternative versions of the retaining fixture are versions that offer a choice between full support or span support of the specimen. If full support is needed, then one can choose a version having slots wide enough to support not only the specimen but also a solid backing plate.
• To some extent, by partially enclosing the specimen, the retaining fixture provides some protection of the furnace insulation and heating elements against flying debris from a specimen and projectile. Shielding separate from the retaining fixture can added in cases in which more protection is needed.
• The rotational stage enables adjustment of the angle of impact — a feature that is desirable for impact testing of vanes under realistic conditions. Alternatively or in addition, if the retaining fixture is of the two-specimen type described above, then the rotational stage can be used to expose both specimens in succession without removing them from the furnace.
• The provision for inserting and removing specimens through the opening in the bottom of the furnace eliminates the need to cool and reheat the furnace between tests, thereby saving substantial amounts of test time.
• When multiple impacts at different positions along a lengthened specimen are required, the retaining fixture can be modified to lengthen the tapered slots and side holes at the additional impact positions, and the linear actuator can be used to place the specimen at the various impact positions. In such a case, the modifications can reduce the shielding effect of the retaining fixture, thereby making it desirable to add separate shielding as mentioned above.

This work was done by Ralph J. Pawlik and Sung R. Choi of **Glenn Research Center***. Further information is contained in a TSP (see page 1).*

Inquiries concerning rights for the commercial use of this invention should be addressed to NASA Glenn Research Center, Innovative Partnerships Office, Attn: Steve Fedor, Mail Stop 4–8, 21000 Brookpark Road, Cleveland, Ohio 44135. Refer to LEW-17610-1.
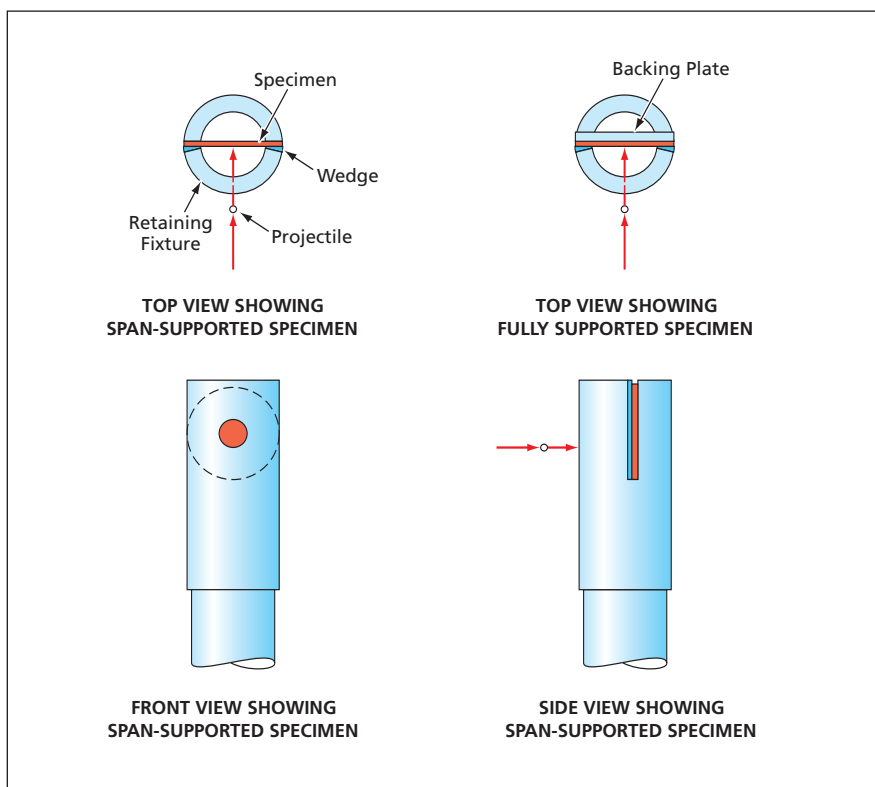
Figure 2. The **Specimen Is Held on the Retaining Fixture** by means of wedges in tapered slots. The slots can be dimensioned to provide span support of the specimen or to accommodate a backing plate for full support of the specimen.

Instrument for Aircraft-Icing and Cloud-Physics Measurements
Data on cloud water content are deduced from hot-wire power levels.

John H. Glenn Research Center, Cleveland, Ohio

The figure shows a compact, rugged, simple sensor head that is part of an instrumentation system for making measurements to characterize the severity of aircraft-icing conditions and/or to perform research on cloud physics. The quantities that are calculated from measurement data acquired by this system and that are used to quantify the severity of icing conditions include sizes of cloud water drops, cloud liquid water content (LWC), cloud ice water content (IWC), and cloud total water content (TWC).

The sensor head is mounted on the outside of an aircraft, positioned and oriented to intercept the ambient airflow. The sensor head consists of an open housing that is heated in a controlled manner to keep it free of ice and that contains four hot-wire elements. The hot-wire sens-

The **Sensor Head** (top) contains three hot-wire sensors oriented perpendicularly to the axis of the tube (across the flow) and one parallel to the axis of the tube (along the flow). The general views of the cockpit display and the sensor are shown, respectively, in the middle and bottom images.

ing elements have different shapes and sizes and, therefore, exhibit different measurement efficiencies with respect to droplet size and water phase (liquid, frozen, or mixed). Three of the hot-wire sensing elements are oriented across the airflow so as to intercept incoming cloud water. For each of these elements, the LWC or TWC affects the power required to maintain a constant temperature in the presence of cloud water.

Each of these three elements is considered to be subject to two forms of heat loss. The first form consists primarily of convective loss attributable to the flow of air past the element. This form is sometimes termed the "dry" loss because it excludes the cooling effect of the impinging water. The second form of heat loss is the cooling effect of impinging water. When the element intercepts liquid cloud water, energy is lost from the element in heating the water from ambient temperature to the equilibrium temperature for evaporation, and further energy is lost as latent heat of vaporization. When the element intercepts cloud ice crystals, there is an additional loss consisting of the latent heat of fusion for melting the ice. In operation, each element is maintained at a temperature of 140 °C by a digital electronic feedback control subsystem. The power expended in maintaining this constant temperature is the measurement datum associated with the element.

The fourth hot-wire sensing element, denoted the reference element, is oriented along the direction of airflow so that it does not intercept cloud water but is still subject to convective cooling. Like the other three elements, the reference element is maintained at constant tem-

perature. In the case of this element, the power needed to maintain the constant temperature is a measure of the dry heat loss and is thus termed the "dry" power. The cloud water content is estimated in a first-principles computation based on known relationships among the cloud water content, the hot-wire power levels, the dimensions of the sensor wires, ambient temperature, and true airspeed.

The measurements and computations needed to quantify cloud IWC (glaciation) and droplet size are more complex. It has long been known that the response of a hot-wire sensor to water droplets decreases with increasing droplet diameter. The response of a wider element is similar to that of a narrower element, except that the onset of the decrease occurs at a larger drop size. Although this droplet-size dependence is not fully theoretically understood, it is empirically known to be highly repeatable and to be useful as a means of inferring droplet diameter: Specifically, measurement data acquired under known conditions in a wind tunnel can be used to calibrate an instrumentation system like this one to enable determination of the median volume diameter of cloud water droplets, given the differences among the responses of the hot-wire sensing elements.

Advances in Measurement of Skin Friction in Airflow

This system implements a combination of established experimental techniques and advanced image processing.

Ames Research Center, Moffett Field, California

The surface interferometric skin-friction (SISF) measurement system is an instrument for determining the distribution of surface shear stress (skin friction) on a wind-tunnel model. The SISF system utilizes the established oil-film interference method, along with advanced image-data-processing techniques and mathematical models that express the relationship between interferograms and skin friction, to determine the distribution of skin friction over an observed region of the surface of a model during a

single wind-tunnel test.

In the oil-film interference method, a wind-tunnel model is coated with a thin film of oil of known viscosity and is illuminated with quasi-monochromatic, collimated light, typically from a mercury lamp. The light reflected from the outer surface of the oil film interferes with the light reflected from the oil-covered surface of the model. In the present version of the oil-film interference method, a camera captures an image of the illuminated model and the image in the cam-

era is modulated by the interference pattern. The interference pattern depends on the oil-thickness distribution on the observed surface, and this distribution can be extracted through analysis of the image acquired by the camera.

The oil-film technique is augmented by a tracer technique for observing the streamline pattern. To make the streamlines visible, small dots of fluorescent-chalk/oil mixture are placed on the model just before a test. During the test, the chalk particles are embedded in the

oil flow and produce chalk streaks that mark the streamlines.

The instantaneous rate of thinning of the oil film at a given position on the surface of the model can be expressed as a function of the instantaneous thickness, the skin-friction distribution on the surface, and the streamline pattern on the surface; the functional relationship is expressed by a mathematical model that is nonlinear in the oil-film thickness and is known simply as the thin-oil-film equation. From the image data acquired as described, the time-dependent oil-thickness distribution and streamline pattern are extracted and by inversion of the

thin-oil-film equation it is then possible to determine the skin-friction distribution.

In addition to a quasi-monochromatic light source, the SISF system includes a beam splitter and two video cameras equipped with filters for observing the same area on a model in different wavelength ranges, plus a frame grabber and a computer for digitizing the video images and processing the image data. One video camera acquires the interference pattern in a narrow wavelength range of the quasi-monochromatic source. The other video camera acquires the streamline image of fluorescence from the chalk in a nearby

but wider wavelength range. The interference-pattern and fluorescence images are digitized, and the resulting data are processed by an algorithm that inverts the thin-oil-film equation to find the skin-friction distribution.

This work was done by James L. Brown of **Ames Research Center** *and Jonathan W. Naughton of MCAT, Inc. Further information is contained in a TSP (see page 1).*

This invention has been patented by NASA (U.S. Patent No. 5,963,310). Inquiries concerning rights for the commercial use of this invention should be addressed to the Ames Technology Partnerships Division at (650) 604-2954. Refer to ARC-14189-1.

Improved Apparatus for Testing Monoball Bearings
Automated tests can be performed over wide ranges of conditions.
Marshall Space Flight Center, Alabama

A desk-sized apparatus for testing monoball bearings and their lubricants offers advantages, relative to prior such apparatuses, of (1) a greater degree of automation and (2) capability of operation under wider and more realistic ranges of test conditions. The ranges of attainable test conditions include load from 100 to >50,000 lb (445 to >2.22 × 10^5 N), resisting torque up to 30,000 lb-in. (≈3,390 N-m),

oscillating rotation through an angle as large as 280°, and oscillation frequency from 0 to 6 Hz. With addition of some components and without major modification of the apparatus, it is also possible to perform tests under environmental conditions that include temperature from –320 to 1,000 °F (–196 to +538 °C), relative humidity from 0 to 100 percent, and either air at ambient pressure, high vacuum, or an atmosphere of monatomic oxygen.

In the apparatus (see Figure 1), a monoball bearing specimen is driven in oscillating rotation by a hydraulic rotary actuator through a series of shafts, one of which incorporates a torque meter and one of which is a flexible coupling. The torque meter measures the resisting torque; the flexible coupling accommodates misalignment, wear, and compression of the specimen and ensures equal loading on opposite sides of the monoball. Not shown in the figure is an angular-position sensor that is used for measuring the angle of rotation of the shafts.

The bearing surfaces that mate with the monoball are supported by an angle plate on one side of the monoball and a trolley on the opposite side. The trolley is supported by very-low-friction cam rollers on its bottom and sides to allow motion in the loading direction only. Rigid side supports absorb the side loads transmitted by the cam rollers. On the opposite end of the trolley from the specimen is a compression load cell, which measures the load, applied by a hydraulic cylinder via a piston that bears against the load cell.
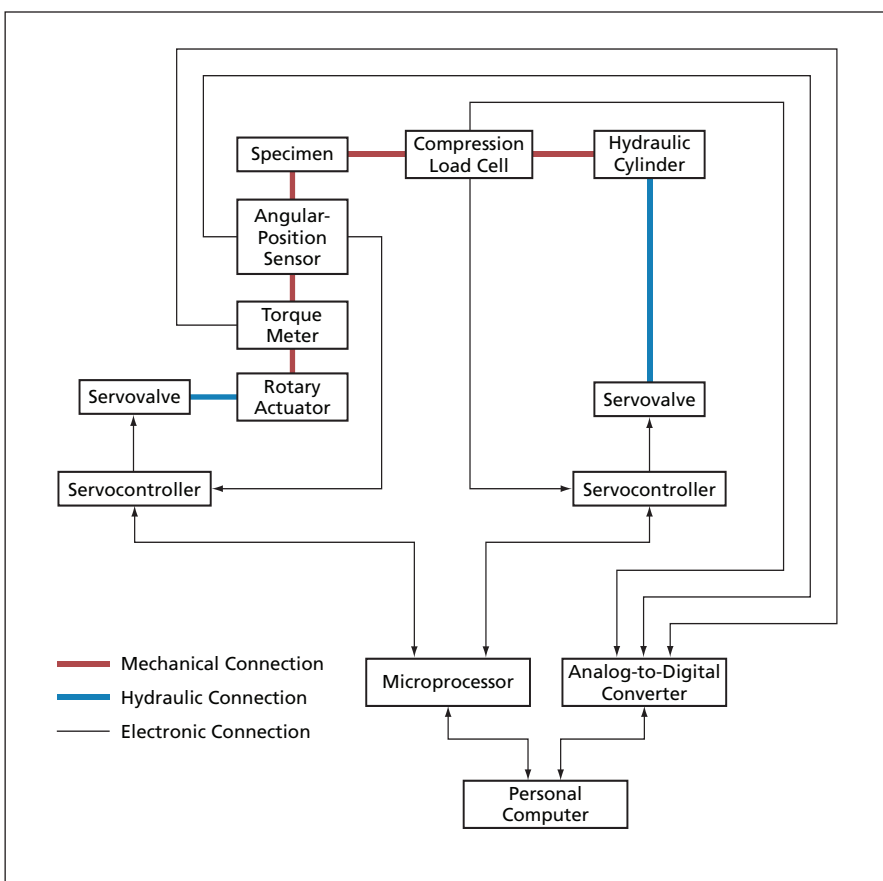
Figure 2. The **Data-Acquisition-and-Control System** of the testing apparatus automates all aspects of testing and processing of test data, once a human operator has initiated a test.
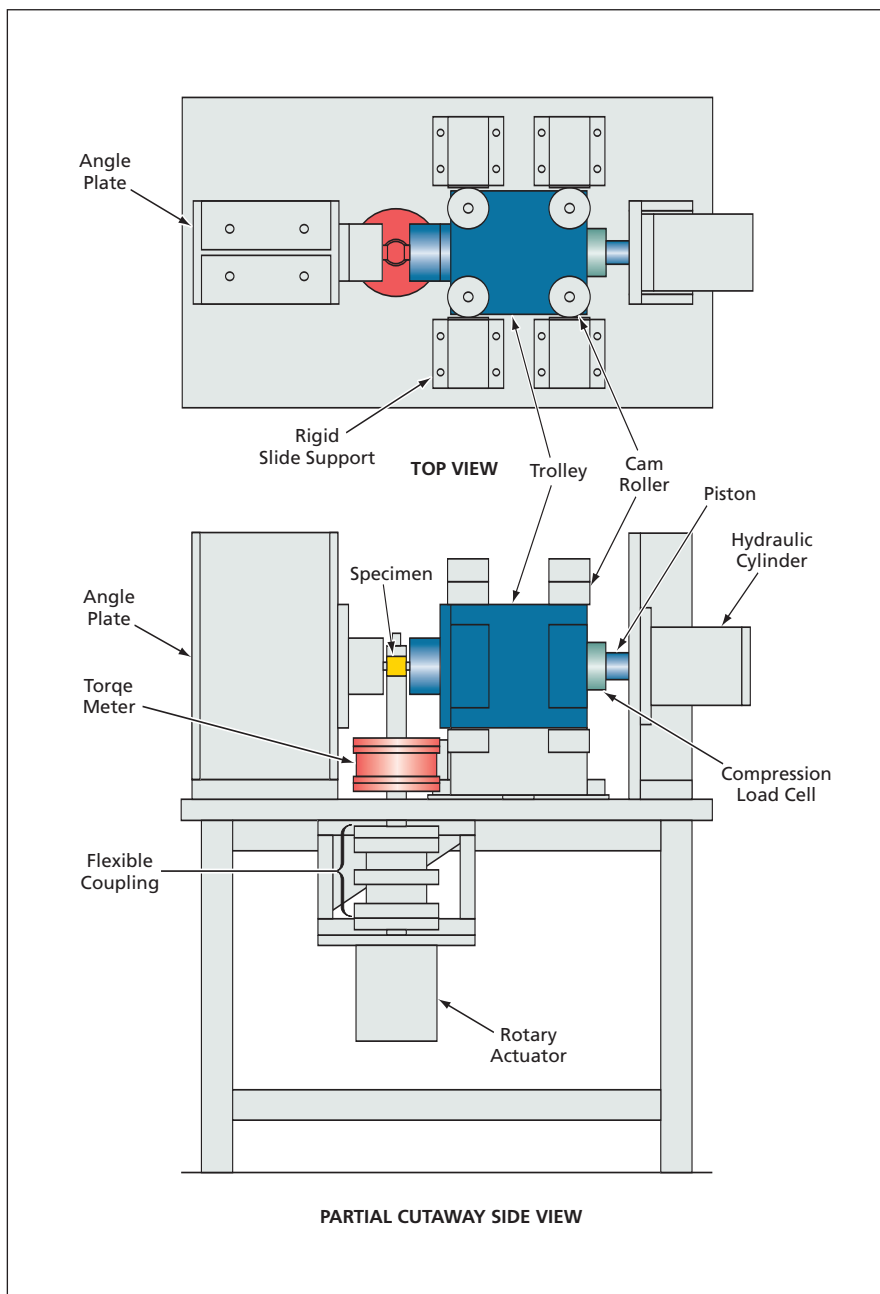
Figure 1. This **Monoball-Bearing-Testing** apparatus subjects a specimen to oscillating rotation at a controlled frequency and amplitude and to a controlled load perpendicular to the axis of rotation.

The apparatus includes a data-acquisition-and-control system (see Figure 2), based on a personal computer and a microprocessor, that controls a test from beginning to end and calculates, displays, and stores test information. An operator enters test instructions into the personal computer, which runs software that translates the instructions into commands. The microprocessor transmits the commands to electronic servocontrollers. Once the operator has initiated a test by entering the instructions, no further intervention by the operator is necessary to ensure successful completion of the test.

The servocontrollers control servovalves that, in turn, control pressures and flows of hydraulic fluids in the hydraulic rotary actuator and the load-applying hydraulic cylinder. Digital signals generated by sensors are fed back to the microprocessor; analog signals from sensors and actuators are fed back to the computer via a fast analog-to-digital converter, and the computer relays these signals to the microprocessor if so required by the test instructions.

The signals from the compression load cell, the torque meter, and the angular-position sensor are used by the control system as both control feedback signals and data. The apparatus measures the applied load, the resisting torque, and the angle of rotation, and the computer calculates the number of cycles and the coefficient of friction in real time. The data are also stored for postprocessing.

✿ High-Speed Laser Scanner Maps a Surface in Three Dimensions
Surface flaws can be scanned automatically and displayed in real time.

Ames Research Center, Moffett Field, California

A scanning optoelectronic instrument generates the digital equivalent of a three-dimensional (X,Y,Z) map of a surface that spans an area with resolution on the order of 0.005 in. (≈0.125mm). Originally intended for characterizing surface flaws (e.g., pits) on space-shuttle thermal-insulation tiles, the instrument could just as well be used for similar purposes in other settings in which there are requirements to inspect the surfaces of many objects. While many commercial instruments can perform this surface-inspection function, the present instrument offers a unique combination of capabilities not available in commercial instruments.

This instrument utilizes a laser triangulation method that has been described previously in *NASA Tech Briefs* in connection with simpler related instruments used for different purposes. The instrument includes a sensor head comprising a monochrome electronic camera and two lasers. The camera is a high-resolution

unit with digital output. The sensor head is mounted on a computer-controlled, servomotor-actuated translation stage at a fixed height above the nominal X,Y plane. Scanning is effected by using the translation stage to position the sensor head repeatedly at small, equal increments of Y until the entire surface has been traversed in the Y dimension.

Figure 1 depicts the basic optical layout for the laser triangulation. The camera is aimed downward (in the –Z direction). Each laser is equipped with optics to project an X-oriented line onto the nominal X,Y plane at a nominal Y position, and is tilted at a known angle of incidence. At each incremental position along the scan, the camera records the image of the laser-illuminated line on the surface. The camera is oriented so that pixel rows are X-oriented and pixel columns are Y-oriented.

The X coordinate of each surface point in the image of the line is obtained by direct correspondence between X and the pixel-column number. Any deviation of the laser-illuminated line from its nominal Y position (and, hence, its nominal pixel-row number) indicates a deviation of the surface from the nominal X,Y plane. The image is digitized and the depth (Z) of the surface at each point along the line is calculated from the Y (pixel-row) deviation by use of a standard triangulation equation. The Y position of each point along the line is obtained from a combination of (1) the known Y position along the scan, (2) the aforementioned Y deviation of the illuminated line, and (3) another standard triangulation equation to correct for the effect of Z on the apparent Y position. The process as described thus far is repeated at each increment of position along the scan. The data collected at all the increments of position are assembled to produce a three-dimensional (3D) map of the surface.

Two lasers are used (but not simultaneously) in conjunction with a dual-scan scheme to overcome shadowing at overhangs, edges of steep holes, and the like. As depicted in the lower part of Figure 1, a surface is scanned twice: from left to right and from right to left. During the scan toward the right, the left laser is used; during the scan toward the left, the right laser is used. Both lasers illuminate common areas (typically, a central area at the bottom of a hole), and each laser illuminates an edge area that may be shaded from the other laser. Surface points in the hole that may be shaded from the left laser during the rightward scan are illuminated by the right laser during the leftward scan, and vice versa.

OPTICAL LAYOUT
(FOR CLARITY, SECOND LASER OMITTED FROM THIS VIEW)

TYPICAL CAMERA IMAGE OF LASER-ILLUMINATED LINE THAT PASSES THROUGH HOLE
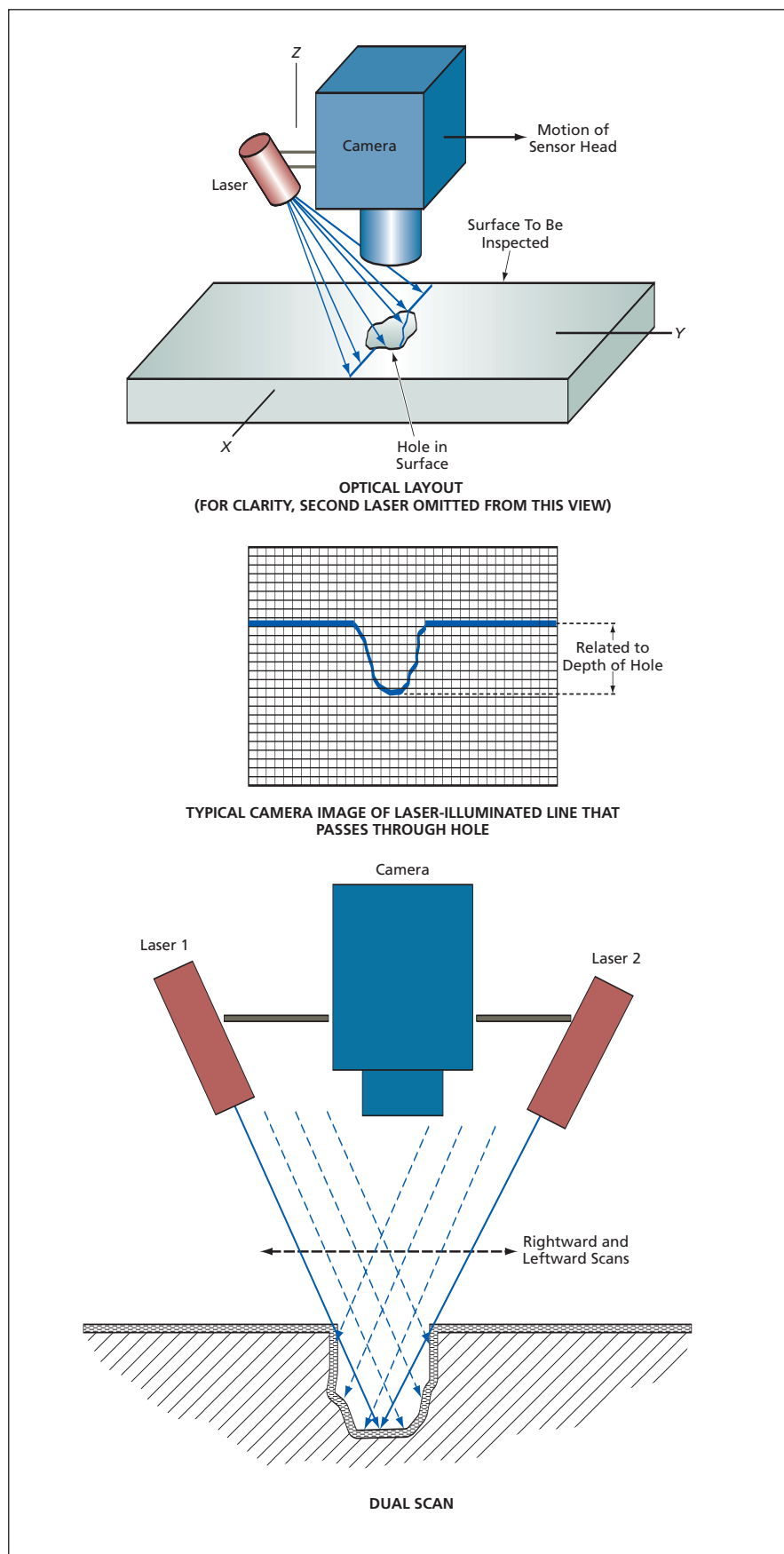
DUAL SCAN

Figure 1. The **Camera Observes the Line of Light** projected on the surface of a plate by a tilted laser. Any deviation of the line from its nominal position is indicative of a hole or bump on the surface.

Figure 2 is a block diagram of the electronic system of the instrument. The system includes an onboard processor, plus an external personal computer (PC) for further processing of the acquired data and displaying resulting depth maps. The processor is capable of generating 3D data in real time, eliminating the need for both onboard memory and post-processing to generate 3D data. The 3D data output of the onboard processor is sent to the PC via a high-speed serial data-communication link. By reducing the computational burden on the PC, onboard preprocessing enables the PC to create and display 3D images in real time during scanning.

*This work was done by Joseph Lavelle and Stefan Schuet of **Ames Research Center**.*

⚙ Electro-Optical Imaging Fourier-Transform Spectrometer
Size, weight, and vibration are reduced by eliminating moving parts.

NASA's Jet Propulsion Laboratory, Pasadena, California

An electro-optical (E-O) imaging Fourier-transform spectrometer (IFTS), now under development, is a prototype of improved imaging spectrometers to be used for hyperspectral imaging, especially in the infrared spectral region. Unlike both imaging and non-imaging traditional Fourier-transform spectrometers, the E-O IFTS does not contain any moving parts. Elimination of the moving parts and the associated actuator mechanisms and supporting structures would increase reliability while enabling reductions in size and mass, relative to traditional Fourier-transform spectrometers that offer equivalent capabilities. Elimination of moving parts would also eliminate the vibrations caused by the motions of those parts.

Figure 1 schematically depicts a traditional Fourier-transform spectrometer, wherein a critical time delay is varied by translating one the mirrors of a Michelson interferometer. The time-dependent optical output is a periodic representation of the input spectrum. Data characterizing the input spectrum are generated through fast-Fourier-transform (FFT) post-processing of the output in conjunction with the varying time delay.

In the E-O IFTS, the Michelson interferometer optics and the bulky, slow translation mechanism are replaced with a solid-state time-delay/interferometer assembly. Included in the assembly (see Figure 2) are an input polarizer, an input passive quarter-wave plate (phase shifter), a series of N liquid-crystal-based electro-optical achromatic half-wave switches (S_1, S_2, . . . S_N) interspersed with a series of $(N + 1)$ passive birefringent wave retarders (Γ_1, Γ_2, . . . Γ_N), and an output polarizer.

The assembly can be regarded as consisting largely of a series of overlapping building blocks, each consisting of two of the passive wave retarders and the achromatic half-wave switch between them. By electro-optically rotating the orientation of the switch to an angle of either 0° or 45° with respect to the input polarization, one can cause the total retardation of the waves passing through the unit to be either the difference or the sum, respectively, of the retardations introduced by the individual retarders. Each retarder following the first one is made twice as thick as (to introduce twice the retardation of) the one
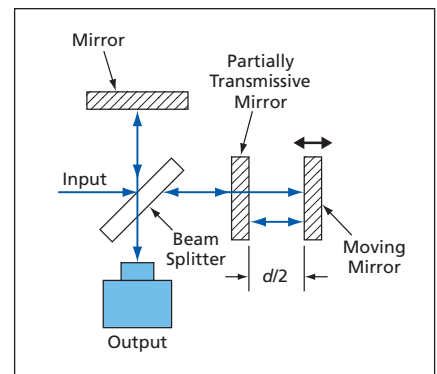
Figure 1. A **Traditional Fourier-Transform Spectrometer** includes a Michelson interferometer in which a time delay d/c (where c is the speed of light) is varied by varying the distance $d/2$ between two mirrors.

preceding it. Hence, by means of binary actuation of the switches among all combinations of sums and differences, it is possible to obtain 2^N different retardation values in increments of the smallest such value and thereby to obtain an arithmetic progression of small time-delay steps.

*This work was done by Tien-Hsin Chao and Hanying Zhou of Caltech for **NASA's Jet Propulsion Laboratory**. Further information is contained in a TSP (see page 1).*
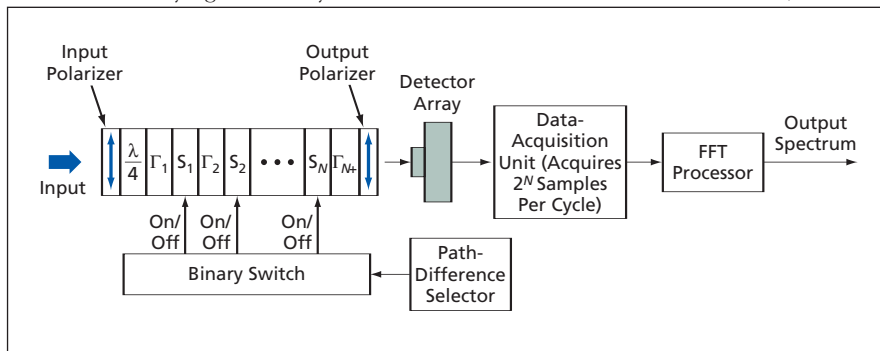
Figure 2. The **E-O IFTS** is built around a solid-state time-delay/interferometer assembly that contains no moving parts.

Infrared Instrument for Detecting Hydrogen Fires

Spatial information is utilized to discriminate against reflected light from other sources.

John F. Kennedy Space Center, Florida

The figure shows an instrument incorporating an infrared camera for detecting small hydrogen fires. The instrument has been developed as an improved replacement for prior infrared and ultraviolet instruments used to detect hydrogen fires. The need for this or any such instrument arises because hydrogen fires (e.g., those associated with leaks from tanks, valves, and ducts) pose a great danger, yet they emit so little visible light that they are mostly undetectable by the unaided human eye. The main performance advantage offered by the present instrument over prior hydrogen-fire-detecting instruments lies in its greater ability to avoid false alarms by discriminating against reflected infrared light, including that originating in (1) the Sun, (2) welding torches, and (3) deliberately ignited hydrogen flames (e.g., ullage-burn-off flames) that are nearby but outside the field of view intended to be monitored by the instrument.

Like prior such instruments, this instrument is based mostly on the principle of detecting infrared emission above a threshold level. However, in addition, this instrument utilizes information on the spatial distribution of infrared light from a source that it detects. Because the combination of spatial and threshold information about a flame tends to constitute a unique signature that differs from that of reflected infrared light originating in a

source not in the field of view, the incidence of false alarms is reduced substantially below that of related prior threshold-based instruments.

The camera in the present instrument is a palm-sized commercial one wherein the image sensor is an array of microbolometers that are sensitive in the wavelength range from 7.5 to 13.5 μm. The camera includes circuitry that preprocesses the microbolometer readings to generate digital output. The camera output is coupled to an embedded image-processing computer via a high-speed serial data interface, conforming

A **Commercial Explosion-Proof Housing** contains the electronic circuitry of the instrument. The housing is fitted with a 2-in. (5.08-cm) germanium window for the infrared camera, and with a pressure port and pressure gauge so that the interior of the housing can be pressurized with inert gas for additional safety in a hazardous environment.

to standard 1394 of the Institute of Electrical and Electronics Engineers (FireWire). The instrument includes a custom circuit board designed to act as interface between (1) the rest of the instrument and (2) external power supplies and external electronic instrumentation and alarm circuits, such that from the perspective of the external instrumentation and alarm circuits, this instru-

ment exactly mimics an older ultraviolet-based hydrogen-fire-detecting instrument to be replaced.

This work was done by Robert Youngquist and Curtis Ihlefeld of **Kennedy Space Center** *and Christopher Immer, Rebecca Oostdyk, Robert Cox, and John Taylor of ASRC Aerospace Corp. Further information is contained in a TSP (see page 1).*
*KSC-12845*

Modified Coaxial Probe Feeds for Layered Antennas

Coaxial shields are connected to radiator and ground planes at standing-wave nodes.

Lyndon B. Johnson Space Center, Houston, Texas

In a modified configuration of a coaxial probe feed for a layered printed-circuit antenna (e.g., a microstrip antenna), the outer conductor of the coaxial cable extends through the thickness of at least one dielectric layer and is connected to both the ground-plane conductor and a radiator-plane conductor. This modified configuration simpli-

fies the incorporation of such radio-frequency integrated circuits as power dividers, filters, and low-noise amplifiers. It also simplifies the design and fabrication of stacked antennas with aperture feeds.

It is often desirable to incorporate the aforementioned integrated circuits into antenna structures in order to obtain better performance or more compact

packaging than would be achievable by packaging these circuits as electrically connected but structurally separate units. In a typical conventional coaxial probe feed configuration, the integrated circuitry is located beneath the ground plane. Incorporation of the integrated circuitry into the antenna entails difficulty in (1) making solder connections

at locations that are partly or totally inaccessible and (2) ensuring the necessary precise alignments between hidden coupled transmission lines. In contrast, in the modified configuration, the integrated circuitry is mounted on the outside, where it is visible and accessible.

The figure shows examples of simple conventional and modified coaxial probe feeds. In the example of the conventional configuration, the outer conductor of a coaxial cable is connected to, and terminated at, a ground-plane metal layer, while the central conductor extends through a single dielectric layer to a connection with a patterned metal radiator element (e.g., a microstrip patch).

In the example of the modified configuration, the outer conductor of the coaxial cable extends through the thickness of the dielectric layer between, and is electrically connected to, both the ground-plane metal conductor and the patterned metal layer on the radiator plane. The central conductor of the coaxial cable extends through the thickness of the dielec-

tric substrate of an integrated circuit to the integrated circuit, which is located on the outer surface. The integrated circuit then excites the cavity formed by the bounding top and bottom planes, by means of an electrical connection passing through an aperture in the patterned metal radiator element (see figure).

Although the coaxial outer conductor constitutes a short circuit between the ground and radiator planes, the effect of the short circuit is minimal because care is taken to locate the coaxial intrusion at a node of the standing-wave mode of the antenna electromagnetic field; that is, the effect of the short circuit is minimal because at its chosen location, the electric field is nominally zero in the absence of perturbations. In the ideal case, the diameter of the outer conductor of the coaxial cable would be zero and there would be no perturbations. In reality, the outer conductor has a finite diameter, leading to a slight shift of the resonance frequency of the antenna. However, the resonance frequency is easily adjusted by slightly chang-

ing the length of the antenna.

In some designs, the metal radiator and ground plane are intentionally short-circuited by use of a post at a specified location to shift the resonance frequency by a specified amount. In an application of the modified configuration to such a design, the coaxial intrusion could be substituted for the post.

The modified feed can also be applied to the so-called PIFA (planar inverted-F antenna), which has achieved great popularity due to its compact size. In this application, the coaxial intrusion provides all or part of the required short circuit between the ground plane and the patterned metal layer on the radiator plane.

This work was done by Patrick W. Fink, Andrew W. Chu, Justin A. Dobbins, and Greg Y. Lin of **Johnson Space Center**.

HALF-WAVELENGTH MICROSTRIP ANTENNA WITH CONVENTIONAL COAXIAL PROBE FEED

HALF-WAVELENGTH MICROSTRIP ANTENNA WITH MODIFIED COAXIAL PROBE FEED
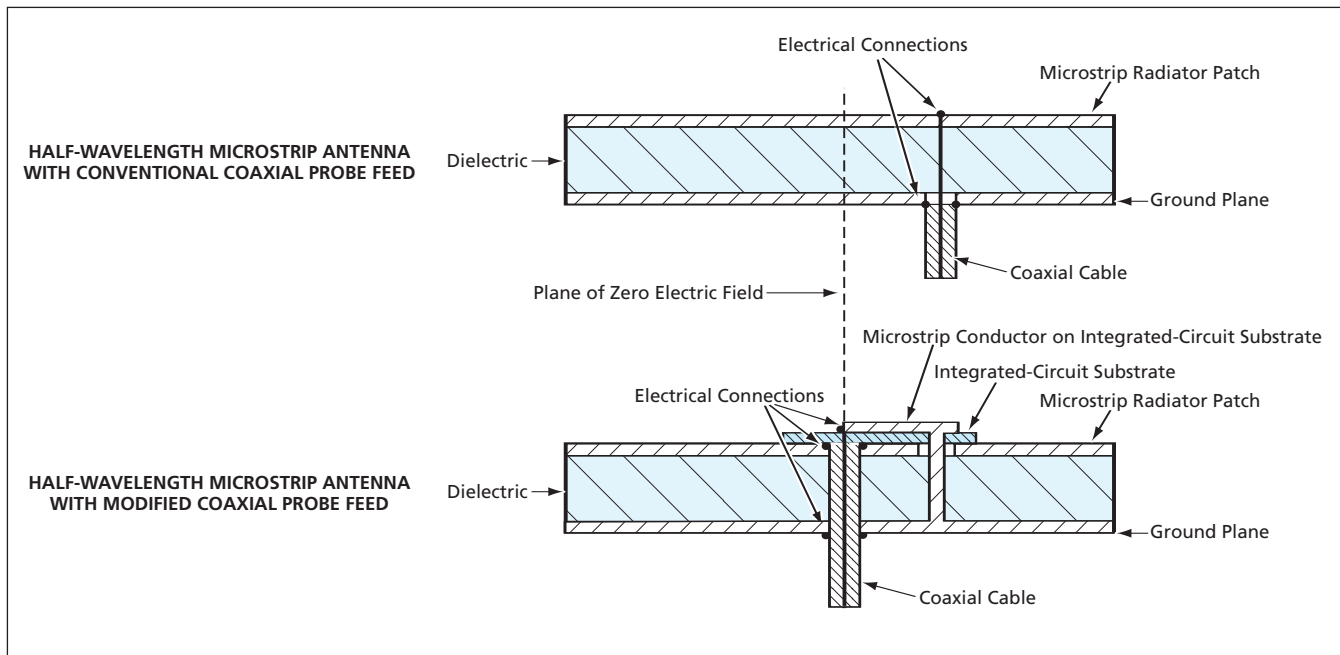
In the **Modified Coaxial Probe Feed**, the outer conductor of the coaxial cable constitutes a short circuit between the ground plane and the radiator patch.

Detecting Negative Obstacles by Use of Radar

Changes in diffraction and reflection would be used to detect abrupt downslopes.

NASA's Jet Propulsion Laboratory, Pasadena, California

Robotic land vehicles would be equipped with small radar systems to detect negative obstacles, according to a proposal. The term "negative obstacles"

denotes holes, ditches, and any other terrain features characterized by abrupt steep downslopes that could be hazardous for vehicles. Video cameras and

other optically based obstacle-avoidance sensors now installed on some robotic vehicles cannot detect obstacles under adverse lighting conditions. Even under fa-

vorable lighting conditions, they cannot detect negative obstacles — at least in part because they cannot see around corners. Other obstacle-avoidance sensors that utilize thermal-infrared radiation from terrain features cannot detect obstacles when temperatures change too rapidly, as they often do at dusk and dawn. The proposed radar systems would not be subject to these limitations.

Radar systems partly similar to the proposed ones are already used in some cars and trucks to warn drivers during backing toward objects that cannot be seen from the drivers' positions. However, those systems are not designed to detect negative obstacles. A radar system according to the proposal would be of the frequency-modulation/continuous-wave (FM/CW) type. It would be installed on a vehicle, facing forward, possibly with a downward slant of the main lobe(s) of the radar beam(s) (see figure). It would utilize one or more wavelength(s) of the order of centimeters.

Because such wavelengths are comparable to the characteristic dimensions of terrain features associated with negative hazards, a significant amount of diffraction would occur at such features. In effect, the diffraction would afford a limited ability to see corners and to see around corners. Hence, the system might utilize diffraction

to detect corners associated with negative obstacles. At the time of reporting the information for this article, preliminary analyses of diffraction at simple negative obstacles had been performed, but an explicit description of how the system would utilize diffraction was not available.

Alternatively or in addition to using diffraction, the system might utilize the Doppler effect and/or the radiation pattern of the radar antenna for detecting negative obstacles. For example, if the forward speed of the vehicle were known, then the approximate direction from the radar apparatus to a reflecting object could be determined from the difference between the Doppler shift of the reflection and the Doppler expected of a reflection from an object straight ahead. For another example, if the main lobe of the radar beam were horizontal or nearly so, then the amount of power reflected from a nearby negative obstacle would be

A **Robotic Vehicle Approaching a Ditch** would carry a radar system that would detect the ditch by recognizing through differences be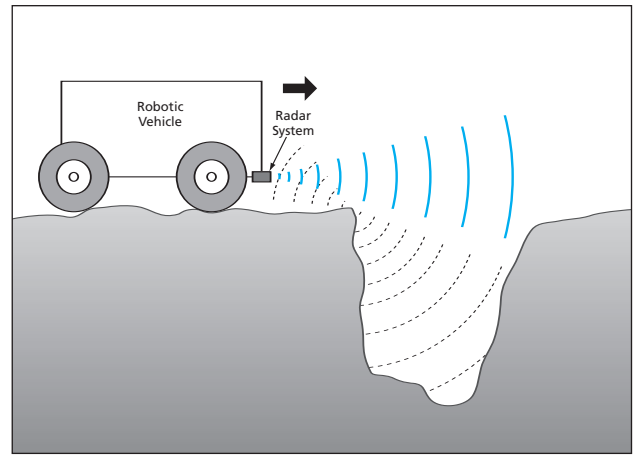tween (1) the signals actually diffracted and reflected and (2) the signals that would be diffracted and reflected from level or nearly level ground.

less than that reflected from level ground at the same horizontal distance from the vehicle. Combining these two examples, it might be possible to detect approaching negative obstacles through changes in the reflected power and/or in the spectral distribution of the reflected power.

This work was done by Anthony Mittskus and James Lux of Caltech for **NASA's Jet Propulsion Laboratory**. *Further information is contained in a TSP (see page 1).*
NPO-40413

Cryogenic Pound Circuits for Cryogenic Sapphire Oscillators
Thermomechanical instabilities and associated frequency instabilities are reduced.

NASA's Jet Propulsion Laboratory, Pasadena, California

Two modern cryogenic variants of the Pound circuit have been devised to increase the frequency stability of microwave oscillators that include cryogenic sapphire-filled cavity resonators. Invented in the 1940s and named after its inventor (R. V. Pound), the original Pound circuit is a microwave frequency discriminator that provides feedback to stabilize a voltage-controlled microwave oscillator with respect to an associated cavity resonator. Heretofore, Pound circuits used in conjunction with cryogenic resonators have included room-temperature electronic components coupled to the resonators via such interconnections as coaxial cables. The thermomechanical instabilities of these interconnections give rise to frequency instabilities. In a cryogenic Pound circuit of the present improved type, all of the active electronic components, the interconnections among them, and the interconnections between them and the resonator re-

side in the cryogenic environment along with the resonator and, hence, are thermomechanically stabilized to a large degree. Hence, further, frequency instabilities are correspondingly reduced.

The active microwave devices required in a Pound circuit are two amplitude detectors and a phase modulator. A Pound circuit generates a frequency-error signal by converting a phase modulation (PM) to an amplitude modulation (AM). The AM in question is generated when a microwave signal that is reflected from a resonator has a high value of the resonance quality factor (Q) and the signal frequency differs from the resonance frequency. A pure PM signal is required because any AM at the input terminal of the resonator would generate a frequency error.

In the present cryogenic Pound circuits (see figure), the active microwave devices are implemented by use of state-of-the-art commercially available tunnel diodes that

exhibit low flicker noise (required for high frequency stability) and function well at low temperatures and at frequencies up to several tens of gigahertz. While tunnel diodes are inherently operable as amplitude detectors and amplitude modulators, they cannot, by themselves, induce significant phase modulation. Therefore, each of the present cryogenic Pound circuits includes passive circuitry that transforms the AM into the required PM. Each circuit also contains an AM detector that is used to sample the microwave signal at the input terminal of the high-Q resonator for the purpose of verifying the desired AM null at this point. Finally, each circuit contains a Pound signal detector that puts out a signal, at the modulation frequency, having an amplitude proportional to the frequency error in the input signal. High frequency stability is obtained by processing this output signal into feedback to a voltage-controlled os-

cillator to continuously correct the frequency error in the input signal.

Each of these circuits first generates a carrier-suppressed AM signal and then transforms that signal into PM by use of a bypass from the radio-frequency input that injects a carrier with ≈90° phase shift from the carrier of the AM signal. (If AM carrier suppression is complete, this phase shift is exactly 90°; if incomplete, a phase shift that deviates somewhat from 90° is required.) An approximation of pure PM is obtained via a coarse adjustment of the phase of this bypassed signal, this adjustment being made by use of a mechanical phase shifter. A fine adjustment to increase the accuracy of the approximation is made by varying the DC voltage applied to the modulation diode(s). Once the mechanical phase shifter is adjusted properly, the variation in DC voltage suffices to maintain pure PM.

The two circuits differ in how they generate the carrier-suppressed AM signal. In the first circuit, this involves combining the outputs from two tunnel diodes that are operated as amplitude modulators configured so that both amplitude modulations and carriers are oppositely phased. This functionality is implemented by mounting the diodes in an antisymmetric arrangement that affords the additional benefit of enabling the use of a single modulation signal, superimposed on a single DC bias, as input to both modulator diodes. If the diodes are perfectly matched, then the carrier can be suppressed completely.

The second circuit was developed after extensive tests and modeling of the behaviors of tunnel diodes showed that a nearly-suppressed-carrier AM signal
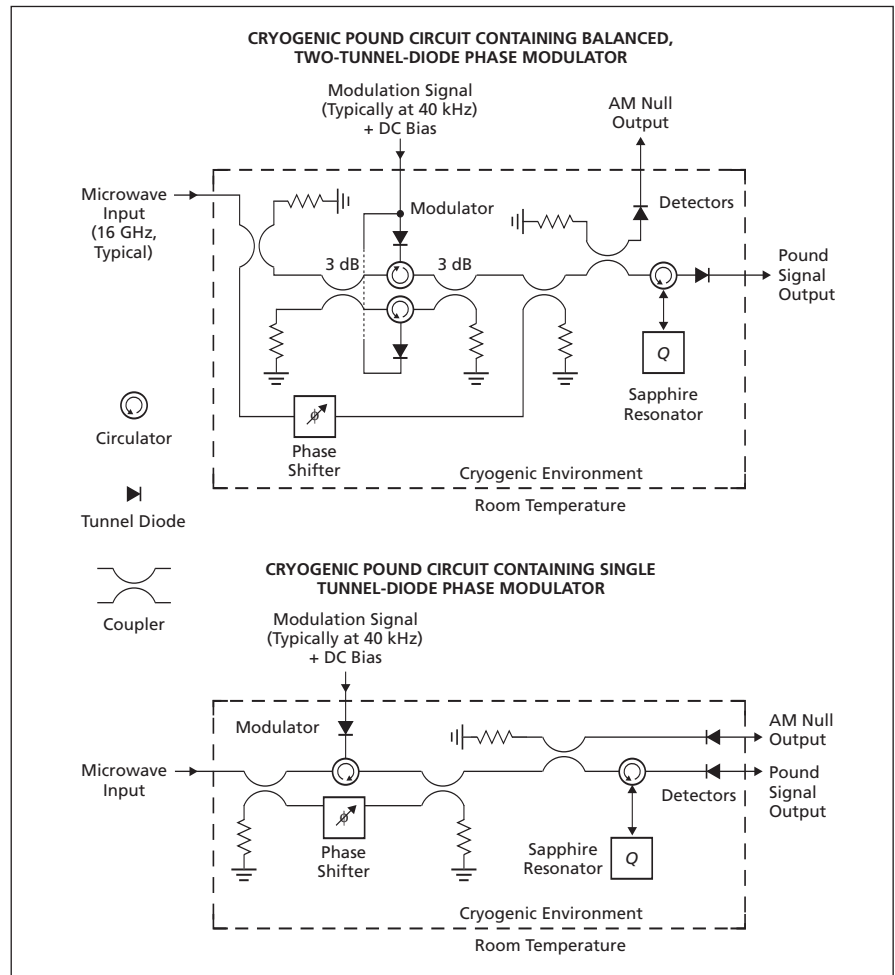
In these **Cryogenic Pound Circuits**, all of the components critical to maintaining frequency stability reside together in the cryogenic environment.

could be generated by use of only one tunnel diode. The obvious advantages of the second circuit, relative to the first one, are fewer components and, consequently, smaller dimensions.

This work was done by G. John Dick and Rabi Wang of Caltech for **NASA's Jet Propulsion Laboratory**. *Further information is contained in a TSP (see page 1). NPO-42172*

Software

PixelLearn

PixelLearn is an integrated user-interface computer program for classifying pixels in scientific images. Heretofore, training a machine-learning algorithm to classify pixels in images has been tedious and difficult. PixelLearn provides a graphical user interface that makes it faster and more intuitive, leading to more interactive exploration of image data sets. PixelLearn also provides image-enhancement controls to make it easier to see subtle details in images. PixelLearn opens images or sets of images in a variety of common scientific file formats and enables the user to interact with several supervised or unsupervised machine-learning pixel-classifying algorithms while the user continues to browse through the images. The machine-learning algorithms in PixelLearn use advanced clustering and classification methods that enable accuracy much higher than is achievable by most other software previously available for this purpose. PixelLearn is written in portable C++ and runs natively on computers running Linux, Windows, or Mac OS X.

The program was written by Dominic Mazzoni, Kiri Wagstaff, Benjamin Bornstein, Nghia Tang, and Joseph Roden of Caltech for **NASA's Jet Propulsion Laboratory**. *Further information is contained in a TSP (see page 1).*

This software is available for commercial licensing. Please contact Karina Edmonds of the California Institute of Technology at (626) 395-2322. Refer to NPO-42082.

New Software for Predicting Charging of Spacecraft

The NASA/Air Force Spacecraft Charging System Analyzer Program (Nascap-2K) is a comprehensive update, revision, and extension of several NASA and Air Force codes for predicting electrical charging of spacecraft. Nascap-2K integrates the capabilities and models included in four independent programs: NASCAP/LEO for low-Earth orbits, NASCAP/GEO for geosynchronous orbits, POLAR for auroral charging in polar orbits, and DynaPAC (Dynamic Plasma Analysis Code) for time-dependent plasma interactions. While each of the earlier codes works well for the range of problems for which it was designed, by today's standards these codes are difficult to learn, cumbersome to use, and overly restrictive in their geometric modeling capabilities. Nascap-2K incorporates these models into a single software package that includes spacecraft surface modeling, spatial gridding, environmental specifications, calculating scripting, and post-processing analysis and visualization. The provided material properties database includes values from earlier programs as well as values from recent measurements. Development of Nascap-2K continues with future capabilities to include interactions with dense plasma such as those produced by electric propulsion.

This work was done by Myron Mandell and Victoria Davis of Science Applications International Corp. (SAIC), and Jeffrey Hilton, formerly of SAIC, for **Marshall Space Flight Center**. *For further information, contact Barbara Gardner at SAIC, Barbara.Gardner@saic.com.*
MFS-31939-1/2056-1

Conversion Between Osculating and Mean Orbital Elements

Osculating/Mean Orbital Element Conversion (C version) (OSMEANC) is a C-language computer program that performs precise conversions between osculating and mean classical orbital elements. OSMEANC can be used for precise design of spacecraft missions and maneuvers and precise calculation of planetary orbits. The program accounts for the full complexity of gravitational fields, including aspherical and third-body effects. In comparison with prior software used for the same purposes, OSMEANC offers greater accuracy in conversion: By virtue of inclusion of high-order gravitational and third-body effects, variations in semimajor axes are calculated to meter-level accuracy. OSMEANC is delivered as a callable shared library. It can be built for any platform with a C compiler. The user interface is via a Python-language wrapper script that can be replaced by the user. OSMEANC is mature and is the product of a significant upgrade from a Fortran version that has been in use since 1991.

This program was written by Joseph Guinn, Min-Kun Chung, and Mark Vincent of Caltech for **NASA's Jet Propulsion Laboratory**. *Further information is contained in a TSP (see page 1).*

This software is available for commercial licensing. Please contact Karina Edmonds of the California Institute of Technology at (818) 393-2827. Refer to NPO-41115.

Generating a 2D Representation of a Complex Data Structure

A computer program, designed to assist in the development and debugging of other software, generates a two-dimensional (2D) representation of a possibly complex n-dimensional (where n is an integer >2) data structure or abstract rank-n object in that other software. The nature of the 2D representation is such that it can be displayed on a non-graphical output device and distributed by non-graphical means. The purpose served by this representation is to assist the user in visualizing and understanding the complex data structure or arbitrarily dimensioned object. This is the only known program that enables a programmer to map an n-dimensional data structure to a flat 2D space. This program does not depend upon the hardware characteristics of a particular output device, and can be executed on a variety of computers from different manufacturers. It can be distributed in source-code or binary-code form. It requires a Lisp compiler. It has no specific memory requirements and depends upon the other software with which it is used and application programs running in it. This software is implemented as a library that is called by, and becomes folded into, the developmental other software.

This work was done by Mark James of Caltech for **NASA's Jet Propulsion Laboratory**. *Further information is contained in a TSP (see page 1).*

This software is available for commercial licensing. Please contact Karina Edmonds of the California Institute of Technology at (818) 393-2827. Refer to NPO-42076.

Making Activated Carbon by Wet Pressurized Pyrolysis

Raw materials other than the traditional ones can now be used.

Ames Research Center, Moffett Field, California

A wet pressurized pyrolysis (wet carbonization) process has been invented as a means of producing activated carbon from a wide variety of inedible biomass consisting principally of plant wastes. The principal intended use of this activated carbon is room-temperature adsorption of pollutant gases from cooled incinerator exhaust streams.

Activated carbon is highly porous and has a large surface area. The surface area depends strongly on the raw material and the production process. Coconut shells and bituminous coal are the primary raw materials that, until now, were converted into activated carbon of commercially acceptable quality by use of traditional production processes that involve activation by use of steam or carbon dioxide.

In the wet pressurized pyrolysis process, the plant material is subjected to high pressure and temperature in an aqueous medium in the absence of oxygen for a specified amount of time to break carbon-oxygen bonds in the organic material and modify the structure of the material to obtain large surface area. Plant materials that have been used in demonstrations of the process include inedible parts of wheat, rice, potato, soybean, and tomato plants. The raw plant material is ground and mixed with a specified proportion of water. The mixture is placed in a stirred autoclave, wherein it is pyrolized at a temperature between 450 and 590 °F (approximately between 230 and 310 °C) and a pressure between 1 and 1.4 kpsi (approximately between 7 and 10 MPa) for a time between 5 minutes and 1 hour.

The solid fraction remaining after wet carbonization is dried, then activated at a temperature of 500 °F (260 °C) in nitrogen gas. The activated carbon thus produced is comparable to commercial activated carbon. It can be used to adsorb oxides of sulfur, oxides of nitrogen, and trace amounts of hydrocarbons, any or all of which can be present in flue gas. Alternatively, the dried solid fraction can be used, even without the activation treatment, to absorb oxides of nitrogen.

*This work was done by John W. Fisher of **Ames Research Center** and Suresh Pisharody, K. Wignarajah, and Mark Moran of Lockheed Martin Corp.*

This invention is owned by NASA and a patent application has been filed. Inquiries concerning rights for the commercial use of this invention should be addressed to the Ames Technology Partnerships Division at (650) 604-2954. Refer to ARC-14929-1.

Composite Solid Electrolyte Containing Li$^+$-Conducting Fibers

Li$^+$-ion conductivities are greater than those achieved before.

John H. Glenn Research Center, Cleveland, Ohio

Improved composite solid polymer electrolytes (CSPEs) are being developed for use in lithium-ion power cells. The matrix components of these composites, like those of some prior CSPEs, are high-molecular-weight dielectric polymers [generally based on polyethylene oxide (PEO)]. The filler components of these composites are continuous, highly-Li$^+$-conductive, inorganic fibers.

PEO-based polymers alone would be suitable for use as solid electrolytes, were it not for the fact that their room-temperature Li$^+$-ion conductivities lie in the range between 10^{-6} and 10^{-8} S/cm — too low for practical applications. In a prior approach to formulating a CSPE, one utilizes nonconductive nanoscale inorganic filler particles to increase the interfacial stability of the conductive phase. The filler particles also trap some electrolyte impurities. The achievable increase in conductivity is limited by the nonconductive nature of the filler particles.
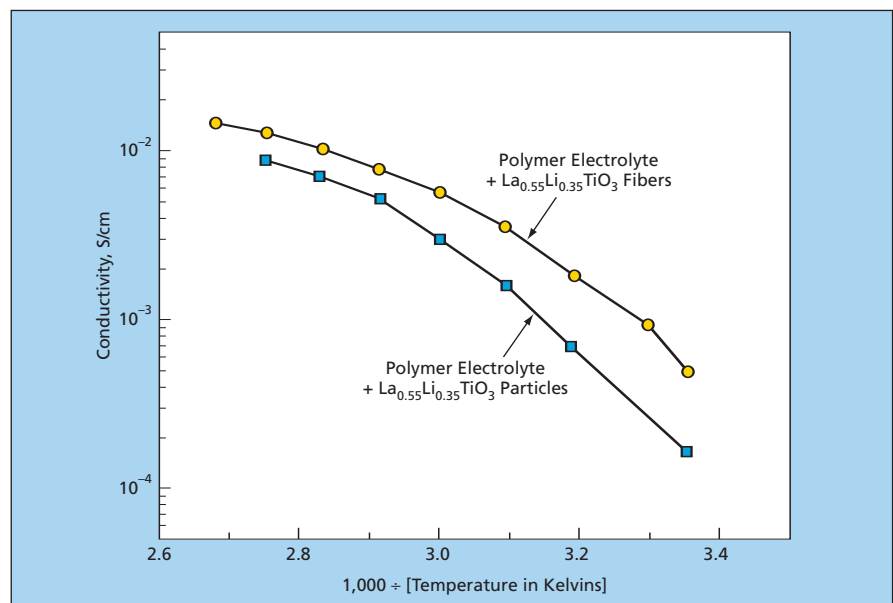
These **Arrhenius Plots** were derived from Li$^+$-ion conductivity measurements on two CSPEs that were identical in the proportions of all ingredients (including the La$_{0.55}$Li$_{0.35}$TiO$_3$ filler), except that in one CSPE, the filler was in particle form, and in the other CSPE , the filler was in fiber form.

In another prior approach — the one leading to the present improved CSPEs — one utilizes a highly-Li$^+$-conductive inorganic filler material to increase the effective Li$^+$-conductivity of the solid electrolyte. In prior CSPE formulations following this approach, the highly-Li$^+$-conductive fillers have been in the form of particles. It has been found that Li$^+$-ion conductivity can be increased to about 10^4 S/cm by use of particles, but that the potential for any further increase is limited by the inherently restrictive nature of contacts between particles.

In contrast, in a CSPE of the present type, interparticle contact or the lack thereof is no longer an issue. In a typical application, a CSPE is formed as a film. The highly-Li$^+$-conductive fibers can penetrate the entire thickness of the film and can thereby effectively constitute a relatively-long-distance Li$^+$-transfer tunnel. The Li$^+$-ion conductivity of the film as a whole is thus increased substantially beyond that achievable by use of particles. For example, the figure presents results of conductivity measurements on two CSPEs made from a PEO-LiN(SO$_2$CF$_2$CF$_3$)$_2$ polymer electrolyte filled with 20 weight percent of the highly-Li$^+$-conductive compound La$_{0.55}$Li$_{0.35}$TiO$_3$.

An additional advantage of using filler fibers is that mechanical properties of the resulting CSPEs are superior to those attainable by use of particle fillers. One disadvantage — at the present state of development — is that relative to particles, fibers are less effective for interface stabilization and trapping of impurities. In contemplated further development, it may be possible to overcome this disadvantage by reducing fiber diameters to the order of nanometers. Other avenues of development could include selection of fiber materials having greater Li$^+$-ion conductivities and finding ways to arrange fibers in velvetlike mats to maximize through-the-thickness conductivities.

This work was done by A. John Appleby, Chunsheng Wang, and Xiangwu Zhang of Texas A&M University for **Glenn Research Center**. *Further information is contained in a TSP (see page 1).*

Inquiries concerning rights for the commercial use of this invention should be addressed to NASA Glenn Research Center, Commercial Technology Office, Attn: Steve Fedor, Mail Stop 4–8, 21000 Brookpark Road, Cleveland, Ohio 44135. Refer to LEW-17470-1.

Electrically Conductive Anodized Aluminum Surfaces

These coatings are highly adherent, transparent, and relatively inexpensive.

Marshall Space Flight Center, Alabama

Anodized aluminum components can be treated to make them sufficiently electrically conductive to suppress discharges of static electricity. The treatment was conceived as a means of preventing static electric discharges on exterior satin-anodized aluminum (SAA) surfaces of spacecraft without adversely affecting the thermal-control/optical properties of the SAA and without need to apply electrically conductive paints, which eventually peel off in the harsh environment of outer space. The treatment can also be used to impart electrical conductivity to anodized housings of computers, medical electronic instruments, telephone-exchange equipment, and other terrestrial electronic equipment vulnerable to electrostatic discharge.

The electrical resistivity of a typical anodized aluminum surface layer lies between 10^{11} and 10^{13} Ω·cm. To suppress electrostatic discharge, it is necessary to reduce the electrical resistivity significantly — preferably to $\leq 10^9$ Ω·cm. The present treatment does this. The treatment is a direct electrodeposition process in which the outer anodized surface becomes covered and the pores in the surface filled with a transparent, electrically conductive metal oxide nanocomposite. Filling the pores with the nanocomposite reduces the transverse electrical resistivity and, in the original intended outer-space application, the exterior covering portion of the nanocomposite would afford the requisite electrical contact with the outer-space plasma.

The electrical resistivity of the nanocomposite can be tailored to a value between 10^7 and 10^{12} Ω·cm. Unlike electrically conductive paint, the nanocomposite becomes an integral part of the anodized aluminum substrate, without need for adhesive bonding material and without risk of subsequent peeling. The electrodeposition process is compatible with commercial anodizing production lines.

At present, the electronics industry uses expensive, exotic, electrostatic-discharge-suppressing finishes: examples include silver impregnated anodized, black electroless nickel, black chrome, and black copper. In comparison with these competing finishes, the present nanocomposite finishes are expected to cost 50 to 20 percent less and to last longer.

This work was done by Trung Hung Nguyen of EIC Laboratories for **Marshall Space Flight Center**. *Further information is contained in a TSP (see page 1). MFS-32092-1*

Rapid-Chill Cryogenic Coaxial Direct-Acting Solenoid Valve

Marshall Space Flight Center, Alabama

A commercially available cryogenic direct-acting solenoid valve has been modified to incorporate a rapid-chill feature. In the original application for which this feature was devised, there is a requirement to ensure that at all times, the valve outlet flow consists entirely or mostly of liquid; that is, there is a requirement to minimize vaporization of cryogenic liquid flowing through the valve. This translates to a requirement to chill interior valve surfaces in contact with the flowing liquid.

The net effect of the modifications is to divert some of the cryogenic liquid to the task of cooling the remainder of the cryogenic liquid that flows to the outlet. Among the modifications are the addition of several holes and a gallery into a valve-seat retainer and the addition of a narrow vent passage from the gallery to the atmosphere. Even when the valve is closed, cryogenic liquid flows from upstream of the valve seat, through the holes, and into the gallery, where it circulates around the valve outlet and may be

partly vaporized before being vented. As a result, the outlet and nearby valve components are maintained at a temperature close to that of the upstream cryogenic liquid. The rate of flow of cryogenic liquid diverted to the task of cooling is limited by the small diameter of the vent passage.

This work was done by James Richard of **Marshall Space Flight Center***, Jim Castor of Castor Engineering, and Richard Sheller of Sverdrup Technology, Inc. Further information is contained in a TSP (see page 1). MFS-32110-1*

Variable-Tension-Cord Suspension/Vibration-Isolation System

Cord tensions are adjusted to optimize vibration-isolation properties.
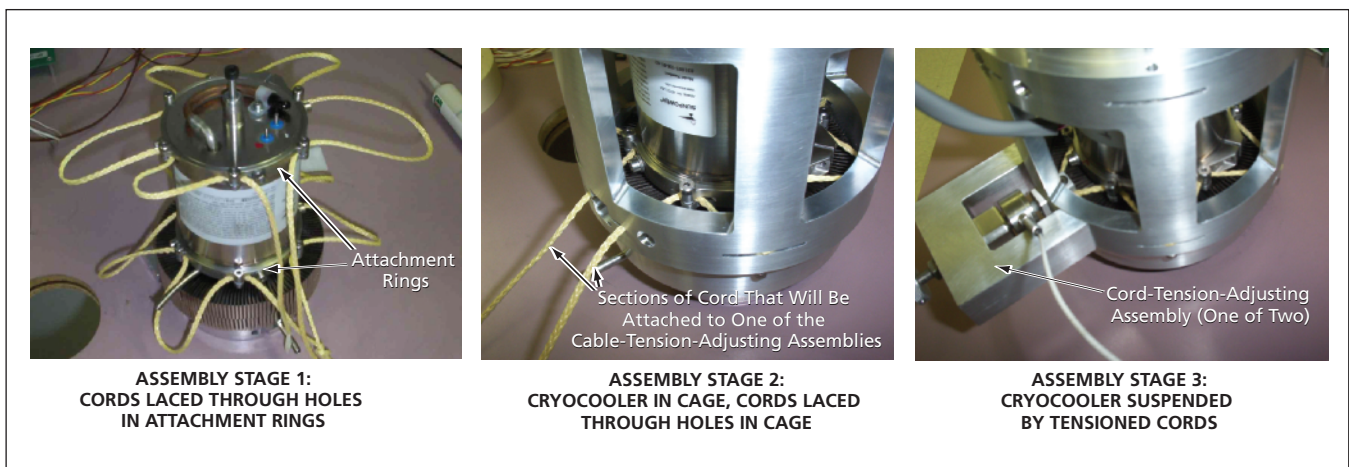
Lyndon B. Johnson Space Center, Houston, Texas

A system for mechanical suspension and vibration isolation of a machine or instrument is based on the use of Kevlar (or equivalent aromatic polyamide) cord held in variable tension between the machine or instrument and a surrounding frame. The basic concept of such a tensioned-cord suspension system (including one in which the cords are made of aromatic polyamide fibers) is not new by itself; what is new here is the additional provision for adjusting the tension during operation to optimize vibration-isolation properties.

In the original application for which

this system was conceived, the objective is to suspend a reciprocating cryocooler aboard a space shuttle and to prevent both (1) transmission of launch vibrations to the cryocooler and (2) transmission of vibrations from the cryocooler to samples in a chamber cooled by the cryocooler. The basic mechanical principle of this system can also be expected to be applicable to a variety of other systems in which there are requirements for cord suspension and vibration isolation.

The reciprocating cryocooler of the original application is a generally axisymmetric object, and the surrounding

frame is a generally axisymmetric object with windows (see figure). Two cords are threaded into a spokelike pattern between attachment rings on the cryocooler, holes in the cage, and cord-tension-adjusting assemblies. Initially, the cord tensions are adjusted to at least the level necessary to suspend the cryocooler against gravitation. Accelerometers for measuring vibrations are mounted (1) on the cold tip of the cryocooler and (2) adjacent to the cage, on a structure that supports the cage. During operation, a technician observes the accelerometer outputs on an oscillo-

ASSEMBLY STAGE 1:
CORDS LACED THROUGH HOLES
IN ATTACHMENT RINGS

Attachment Rings

Sections of Cord That Will Be Attached to One of the Cable-Tension-Adjusting Assemblies

ASSEMBLY STAGE 2:
CRYOCOOLER IN CAGE, CORDS LACED
THROUGH HOLES IN CAGE

Cord-Tension-Adjusting Assembly (One of Two)

ASSEMBLY STAGE 3:
CRYOCOOLER SUSPENDED
BY TENSIONED CORDS

The **Suspension/Vibration-Isolation System** of the original application is depicted here at three successive stages of assembly.

scope while manually adjusting the cord tensions in an effort to minimize the amount of vibration transmitted to and/or from the cryocooler.

A contemplated future version of the system would include a microprocessor-based control subsystem that would include cord-tension actuators. This control subsystem would continually adjust the cord tension in response to accelerometer feedback to optimize vibration-isolation properties as required for various operating conditions. The control system could also adjust cord tensions (including setting the two cords to different tensions) to suppress resonances. Other future enhancements could include optimizing the cord material, thickness, and braid; optimizing the spoke patterns; and adding longitudinal cords for applications in which longitudinal stiffness and vibration suppression are required.

Manufacturing & Prototyping

Techniques for Connecting Superconducting Thin Films

Junctions can be tailored to obtain desired levels of electrical resistance.

Marshall Space Flight Center, Alabama

Several improved techniques for connecting superconducting thin films on substrates have been developed. The techniques afford some versatility for tailoring the electronic and mechanical characteristics of junctions between superconductors in experimental electronic devices. The techniques are particularly useful for making superconducting or alternatively normally conductive junctions (e.g., Josephson junctions) between patterned superconducting thin films in order to exploit electron quantum-tunneling effects.

The techniques are applicable to both low-T_c and high-T_c superconductors (where T_c represents the superconducting-transition temperature of a given material), offering different advantages for each. Most low-T_c superconductors are metallic, and heretofore, connections among them have been made by spot welding. Most high-T_c superconductors are nonmetallic and cannot be spot welded. These techniques offer alternatives to spot welding of most low-T_c superconductors and additional solutions to problems of connecting most high-T_c superconductors.

A superconducting thin film can be formed on a flat substrate. When two such substrate-supported thin films are placed face-to-face in tight contact by any means, electrical conductivity can be established across the resulting interface or junction between them. If the electri-

cal resistance of the junction can be made relatively low, then the junction can serve as an ordinary electrical connection between the superconductors. On the other hand, provided that the junction can be tailored to impart a specified larger electrical resistance, the junction can be used to create desired electron quantum-tunneling effects. Such a thin-film-to-thin-film contact can be formed in one of three ways:

1. Bonding the two substrates together,
2. Mechanically fastening the two substrates together, or
3. Bonding the two thin films together, with or without bonding and/or mechanically fastening of the two substrates.

In general, one would bond the substrates to obtain reliability better than could be obtained by mechanical fastening of the substrates. On the other hand, mechanical fastening of the substrates offers the advantage of reversibility of the connection between the superconducting thin films.

For the purpose of the present innovation, the bonding of substrates and superconducting films can be effected by any of the established techniques generally used for that purpose in the art of superconducting thin films. In particular, the hydroxide catalyzed optical bonding process developed for NASA's Gravity Probe B mission is well-suited for the controlled bonding of superconductors.

Prior to making a junction in one of the three ways described above, the electrical resistance of the junction can be modified in one of the following ways, depending on the specific application:

- Generally, the electrical resistance of the junction can be increased by creating an electrically resistive layer on either or both superconducting thin films to be bonded.
- In the case of metallic superconducting thin films with surface oxide layers, the electrical resistance of the junction can be reduced by etching, scratching, or polishing to thin or remove the oxide layers. In one variant of this approach, the two thin films can simply be scratched against each other while the electrical resistance is monitored in real time to prevent excessive thinning of the oxide.
- If the two superconducting thin films are to be directly bonded, the electrical resistance of the junction can be increased in a controlled manner via the resistance of a bonding material. Optionally, beads of a known electrical resistivity and known size distribution can be added to the bonding material to control the thickness of the bonding interfacial layer and thereby obtain the desired electrical resistance.

Versatile Friction Stir Welding/Friction Plug Welding System

A single system could perform any FSW or FPW operation.

Marshall Space Flight Center, Alabama

A proposed system of tooling, machinery, and control equipment would be capable of performing any of several friction stir welding (FSW) and friction plug welding (FPW) operations. These operations would include the following:

- Basic FSW;
- FSW with automated manipulation

of the length of the pin tool in real time [the so-called auto-adjustable pin-tool (APT) capability];
- Self-reacting FSW (SRFSW);
- SR-FSW with APT capability and/or real-time adjustment of the distance between the front and back shoulders; and

- Friction plug welding (FPW) [more specifically, friction push plug welding] or friction pull plug welding (FPPW) to close out the keyhole of, or to repair, an FSW or SR-FSW weld.

Prior FSW and FPW systems have been capable of performing one or

two of these operations, but none has thus far been capable of performing all of them.

The proposed system would include a common tool that would have APT capability for both basic FSW and SR-FSW. Such a tool was described in "Tool for Two Types of Friction Stir Welding" (MFS-31647-1), *NASA Tech Briefs*, Vol. 30, No. 10 (October 2006), page 70. Going beyond what was reported in the cited previous article, the common tool could be used in conjunction with a plug welding head to perform FPW or FPPW. Alternatively, the plug welding head could be integrated, along with the common tool, into a FSW head that would be capable of all of the aforementioned FSW and FPW operations. Any FSW or FPW operation could be performed under any combination of position and/or force control.

Thermal Spore Exposure Vessels
Thermal masses are minimized to enable rapid heating and cooling.

NASA's Jet Propulsion Laboratory, Pasadena, California

Thermal spore exposure vessels (TSEVs) are laboratory containers designed for use in measuring rates of death or survival of microbial spores at elevated temperatures. A major consideration in the design of a TSEV is minimizing thermal mass in order to minimize heating and cooling times. This is necessary in order to minimize the number of microbes killed before and after exposure at the test temperature, so that the results of the test accurately reflect the effect of the test temperature.

A typical prototype TSEV (see figure) includes a flat-bottomed stainless-steel cylinder 4 in. (10.16 cm) long, 0.5 in. (1.27 cm) in diameter, having a wall thickness of 0.010±0.002 in. (0.254±0.051 mm). Microbial spores are deposited in the bottom of the cylinder, then the top of the cylinder is closed with a sterile rubber stopper. Hypodermic needles are used to puncture the rubber stopper to evacuate the inside of the cylinder or to purge the inside of the cylinder with a gas. In a typical application, the inside of the cylinder is purged with dry nitrogen prior to a test.

During a test, the lower portion of the cylinder is immersed in a silicone-oil bath that has been preheated to and maintained at the test temperature. Test temperatures up to 220 °C have been used. Because the spores are in direct contact with the thin cylinder wall, they quickly become heated to the test temperature.

This work was done by Robert A. Beaudet, Michael Kempf, and Larry Kirschner of Caltech for **NASA's Jet Propulsion Laboratory**. *Further information is contained in a TSP (see page 1). NPO-41091*

A **TSEV** is a test-tube-like stainless-steel vessel that can be purged with a gas and immersed in a hot oil bath.

Enumerating Spore-Forming Bacteria Airborne With Particles
Complementary data are obtained by use of two instruments and correlated.

NASA's Jet Propulsion Laboratory, Pasadena, California

A laboratory method has been conceived to enable the enumeration of
- Cultivable bacteria and bacterial spores that are, variously, airborne by themselves or carried by, parts of, or otherwise associated with, other airborne particles; and
- Spore-forming bacteria among all of the aforementioned cultivable microbes.

The method was originally intended to be used along with other methods as means of quantitative assessment of the potential for contamination of remote planets by bacterial spores carried aboard spacecraft from Earth. There may also be potential terrestrial applications in assessing actual or potential airborne biological contamination on Earth. Of particular interest, for a given sample, the method provides information on the average number of spores per particle as a function of particle size. This information is important for studies of airborne biological contamination because (1) spores are particles and are believed to be associated with other particles and (2) entrainment and transport of particles in air are strongly affected by particle size.

The method involves the use of two commercially available instruments:
- One instrument is a quartz-crystal-microbalance (QCM) ten-stage cascade impactor, which can quantify airborne particles of different sizes but cannot measure bacterial content.
- The other instrument is a particle counter that includes six stages, in which are placed tryptic soy agar (TSA) plates to collect particles in six different size ranges. TSA is a basic medium used for culturing many kinds of microorganisms. This instrument indicates the numbers of microbial colonies that grow on the plates after incubation, which numbers correlate with the numbers of the cultivable total microbes collected in air.

However, this instrument does not count all of the particles (including particles other than bacteria and spores) collected on each agar plate.

The method prescribes two tasks, the first being to determine the total distribution of cultivable microbes (both spore-forming and non-spore-forming) on airborne particles of different sizes. In this first task, the two instruments are positioned side by side and run simultaneously. The six-stage counter gives the total number of cultivable microbes per unit area for each particle size range. The QCM ten-stage cascade impactor gives the total numbers of particles (including particles other than cultivable microbes) per unit area per size range. The size ranges of the two instruments are different. The data acquired by the two instruments are consolidated in a procedure that includes taking account of the differences between the size ranges. This procedure yields information on the average

number of cultivable microbes per particle as a function of particle size.

The second task is to determine the distribution of spore-forming bacteria (and not of non-spore-forming bacteria) on airborne particles of various sizes. This task incorporates the procedures of the first task and includes additional procedures. Because the colonies collected by the six-stage particle counter contain non-spore-forming as well as spore-forming bacteria, this task includes a procedure for differentiating between the spore-forming and non-spore-forming colonies.

To start the differentiation procedure, a sample is taken from every colony on the agar plates and incubated in a nutrient sporulation medium (NSM) for seven days. An NSM is a low-nutrient medium, and only spore-forming species (which are hardier than non-spore-forming species) are capable of forming spores that can survive the week-long low-nutrient condition. Next, the NSM-incubated samples are subjected to a heat shock consisting of a temperature of 80 °C for 15 minutes. Spores can survive the heat shock, but non-spore-forming bacteria and spore-forming bacteria that are not in spore form cannot survive. Therefore, any colonies that resume growth after the incubation in the NSM and the heat shock are deemed to be colonies of spore-forming bacteria. The resulting knowledge of which of the colonies on the agar plates consist of spore-forming bacteria is used to form the counts in the six size ranges, then the data from the two instruments are consolidated, in the same manner as in the first task, to obtain the average number of spore-forming bacteria per particle of each size range.

Miniature Oxidizer Ionizer for a Fuel Cell

NASA's Jet Propulsion Laboratory, Pasadena, California

A proposed miniature device for ionizing the oxygen (or other oxidizing gas) in a fuel cell would consist mostly of a membrane ionizer using the same principles as those of the device described in the earlier article, "Miniature Bipolar Electrostatic Ion Thruster" (NPO-21057). The oxidizing gas would be completely ionized upon passage through the holes in the membrane ionizer. The resulting positively charged atoms or molecules of oxidizing gas could then, under the influence of the fringe fields of the ionizer, move toward the fuel-cell cathode that would be part of a membrane/electrode assembly comprising the cathode, a solid-electrolyte membrane, and an anode. The electro-oxidized state of the oxidizer atoms and molecules would enhance transfer of them through the cathode, thereby reducing the partial pressure of the oxidizer gas between the ionizer and the fuel-cell cathode, thereby, in turn, causing further inflow of oxidizer gas through the holes in the membrane ionizer. Optionally the ionizer could be maintained at a positive electric potential with respect to the cathode, in which case the resulting electric field would accelerate the ions toward the cathode.

This work was done by Frank Hartley of Caltech for **NASA's Jet Propulsion Laboratory**. *Further information is contained in a TSP (see page 1). NPO-21087*

Miniature Ion-Array Spectrometer

## The mode of operation would differ from that described in the preceding article.

NASA's Jet Propulsion Laboratory, Pasadena, California

The figure depicts a proposed miniature ion-mobility spectrometer that would share many features of design and operation of the instrument described in the immediately preceding article. The main differences between that instrument and this one would lie in the configuration and mode of operation of the filter and detector electrodes. A filter electrode and detector electrodes would be located along the sides of a drift tube downstream from the accelerator electrode. These electrodes would apply a combination of (1) a transverse AC electric field that would effect differential transverse dispersal of ions and (2) a transverse DC electric field that would drive the dispersed ions toward the detector electrodes at different distances along the drift tube. The electric current collected by each detector electrode would be a measure of the current, and thus of the abundance of the species of ions impinging on that electrode. The currents collected by all the detector electrodes could be measured simultaneously to obtain continuous readings of abundances of species. The downstream momentum of accelerated ions would be maintained through neutralization on the electrodes; the momentum of the resulting neutral atoms would serve to expel gases from spectrometer, without need for a pump.

The proposed ion-mobility spectrometer would have no moving parts and would be extremely robust. It would consume little power, most of which would be attributable to the ion currents collected by the detector electrodes. The DC-DC converters needed to apply the required voltages and the amplifiers and controllers needed for operation and for processing of detector outputs could be constructed as application-specific integrated circuits. It has been estimated that the entire instrument could fit in a package smaller than a fingernail.

This work was done by Frank T. Hartley of Caltech for **NASA's Jet Propulsion Laboratory**. *Further information is contained in a TSP (see page 1). NPO-21193*
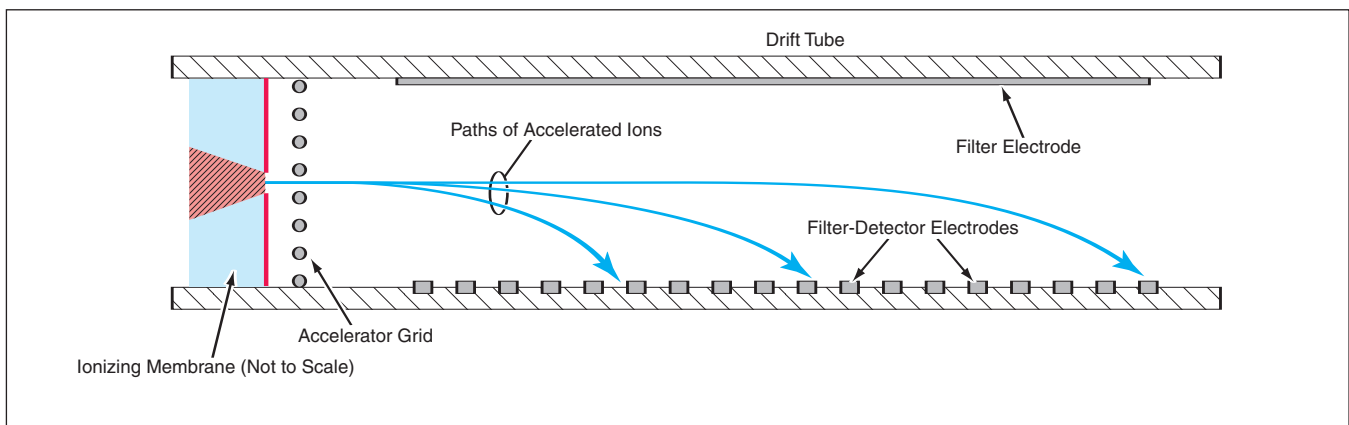
This **Proposed Ion-Mobility Spectrometer** would give continuous readings of ion-species abundances. It would be smaller and simpler relative to prior ion-mobility spectrometers based on pulsed operation and a time-of-flight principle.

Promoted-Combustion Chamber With Induction Heating Coil

Tests can be done at temperature and pressure combinations not previously attainable.

Marshall Space Flight Center, Alabama

An improved promoted-combustion system has been developed for studying the effects of elevated temperatures on the flammability of metals in pure oxygen. In prior promoted-combustion chambers, initial temperatures of metal specimens in experiments have been limited to the temperatures of gas supplies, usually near room temperature. Although limited elevated temperature promoted-combustion chambers have been developed using water-cooled induction coils for preheating specimens, these designs have been limited to low-pressure operation due to the hollow induction coil. In contrast, the improved promoted-combustion chamber can sustain a pressure up to 10 kpsi (69 MPa) and, through utilization of a solid induction coil, is capable of preheating a metal specimen up to its melting point [potentially in excess of 2,000 °F (≈1,100 °C)]. Hence, the improved promoted-combustion chamber makes a greater range of physical conditions and material properties accessible for experimentation.

The chamber consists of a vertical cylindrical housing with an inner diameter of 8 in. (20.32 cm) and an inner height of 20.4 in. (51.81 cm). A threaded, sealing cover at one end of the housing can be unscrewed to gain access for installing a specimen. Inlet and outlet ports for gases are provided. Six openings arranged in a helical pattern in the chamber wall contain sealed sapphire windows for viewing an experiment in progress.

The base of the chamber contains pressure-sealed electrical connectors for supplying power to the induction coil. The connectors feature a unique design that prevents induction heating of the housing and the pressure sealing surfaces; this is important because if such spurious induction heating were allowed to occur, chamber pressure could be lost.

The induction coil is 10 in. (25.4 cm) long and is fitted with a specimen holder at its upper end. At its lower end, the induction coil is mounted on a ceramic base, which affords thermal insulation to prevent heating of the base of the chamber during use. A sapphire cylinder protects the coil against slag generated during an experiment.

The induction coil is energized by a 6-kW water-cooled power supply operating at a frequency of 400 kHz. The induction coil is part of a parallel-tuned circuit, the tuning of which is used to adjust the coupling of power to the specimen.

The chamber is mounted on a test stand along with pumps, valves, and plumbing for transferring pressurized gas into and out of the chamber. In addition to multiple video cameras aimed through the windows encircling the chamber, the chamber is instrumented with gauges for monitoring the progress of an experiment. One of the gauges is a dual-frequency infrared temperature transducer aimed at the specimen through one window. Chamber operation is achieved via a console that contains a computer running apparatus-specific software, a video recorder, and real-time video monitors. For safety, a blast wall separates the console from the test stand.

Miniature Ion-Mobility Spectrometer

Advantages would include robustness, simplicity, and extreme miniaturization.

NASA's Jet Propulsion Laboratory, Pasadena, California

The figure depicts a proposed miniature ion-mobility spectrometer that would be fabricated by micromachining. Unlike prior ion-mobility spectrometers, the proposed instrument would not be based on a time-of-flight principle and, consequently, would not have some of the disadvantageous characteristics of prior time-of-flight ion-mobility spectrometers. For example, one of these characteristics is the need for a bulky carrier-gas-feeding subsystem that includes a shutter gate to provide short pulses of gas in order to generate short pulses of ions. For another example, there is need for a complex device to generate pulses of ions from the pulses of gas and the device is capable of ionizing only a fraction of the incoming gas molecules; these characteristics preclude miniaturization. In contrast, the proposed instrument would not require a carrier-gas-feeding subsystem and would include a simple, highly compact device that would ionize all the molecules passing through it.

The ionization device in the proposed instrument would be a 0.1-micron-thick dielectric membrane with metal electrodes on both sides. Small conical holes would be micromachined through the membrane and electrodes. An electric potential of the order of a volt applied between the membrane electrodes would give rise to an electric field of the order of several megavolts per meter in the submicron gap between the electrodes. An electric field of this magnitude would be sufficient to ionize all the molecules that enter the holes. Ionization (but not avalanche arcing) would occur because the distance between the ionizing electrodes would be less than the mean free path of gas molecules at the operating pressure of instrument.

An accelerating grid would be located inside the instrument, downstream from the ionizing membrane. The electric potential applied to this grid would be negative relative to the potential on the inside electrode of the ionizing membrane and would be of a magnitude sufficient to generate a moderate electric field. Positive ions leaving the membrane holes would be accelerated in this electric field. The resulting flux of ions away from the ionization membrane would create a partial vacuum that would draw more of the gas medium through the membrane.

The figure depicts a filter electrode and detector electrodes located along the sides of a drift tube downstream from the accelerator electrode. These electrodes would apply a transverse AC electric field superimposed on a ramped DC electric
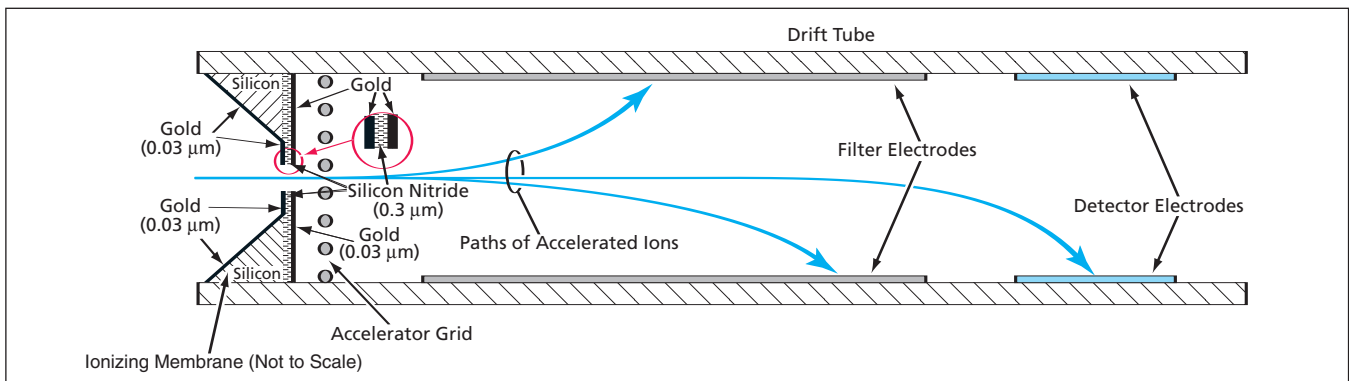
This **Proposed Ion-Mobility Spectrometer** would be made to sweep repeatedly through a spectrum of ionic species by applying a combination of AC and ramped DC voltages between the filter electrodes.

field. The AC field would effect differential transverse dispersal of ions. At a given instant of time, the trajectories of most of the ions would be bent toward the electrodes, causing most of the ions to collide with the electrodes and thereby become neutralized. The DC field would partly counteract the dispersive effect of the AC field, straightening the trajectories of a selected species of ions; the selection would vary with the magnitude of the applied DC field. The straightening of the trajectories of the selected ions would enable them to pass into the region between the detector electrodes. Depending on the polarity of the voltage applied to the detector electrodes, the electric field between the detector electrodes would draw the selected ions to one of these electrodes. Hence, the current collected by one of the detector electrodes would be a measure of the abundance of ions of the selected species. The ramping of the filter-electrode DC voltage would sweep the selection of ions through the spectrum of ionic species.

This work was done by Frank T. Hartley of Caltech for **NASA's Jet Propulsion Laboratory**. *Further information is contained in a TSP (see page 1). NPO-21109*

Mixed-Salt/Ester Electrolytes for Low-Temperature Li⁺ Cells

NASA's Jet Propulsion Laboratory, Pasadena, California

Electrolytes comprising, variously, $LiPF_6$ or $LiPF_6$ plus $LiBF_4$ dissolved at various concentrations in mixtures of alkyl carbonates and alkyl esters have been found to afford improved low-temperature performance in rechargeable lithium-ion electrochemical cells. These and other electrolytes have been investigated in a continuing effort to extend the lower limit of operating temperatures of such cells. This research at earlier stages, and the underlying physical and chemical principles, were reported in numerous previous *NASA Tech Briefs* articles, the most recent being "Ester-Based Electrolytes for Low-Temperature Li-Ion Cells" (NPO-41097), *NASA Tech Briefs*, Vol. 29, No. 12 (December 2005), page 59. The ingredients of the solvent mixtures include ethylene carbonate (EC), ethyl methyl carbonate (EMC), methyl butyrate (MB), and methyl propionate (MP). The electrolytes were placed in Li-ion cells containing carbon anodes and $LiNi_{0.8}Co_{0.2}O_2$ cathodes, and the electrical performances of the cells were measured over a range of temperatures down to –60 °C. The electrolytes that yielded the best low-temperature performances were found to consist, variously, of 1.0 M $LiPF_6$ + 0.4 M $LiBF_4$ or 1.4 $LiPF_6$ in 1EC + 1EMC + 8MP or 1EC + 1EMC + 8MB, where the concentrations of the salts are given in molar units and the proportions of the solvents are by relative volume.

This work was done by Marshall Smart and Ratnakumar Bugga of Caltech for **NASA's Jet Propulsion Laboratory**. *Further information is contained in a TSP (see page 1). NPO-42862*

Miniature Free-Space Electrostatic Ion Thrusters

NASA's Jet Propulsion Laboratory, Pasadena, California

A miniature electrostatic ion thruster is proposed for maneuvering small spacecraft. In a thruster based on this concept, one or more propellant gases would be introduced into an ionizer based on the same principles as those of the device described in the earlier article, "Miniature Bipolar Electrostatic Ion Thruster" (NPO-21057). On the front side, positive ions leaving an ionizer element would be accelerated to high momentum by an electric field between the ionizer and an accelerator grid around the periphery of the concave laminate structure. On the front side, electrons leaving an ionizer element would be ejected into free space by a smaller accelerating field. The equality of the ion and electron currents would eliminate the need for an additional electron- or ion-emitting device to keep the spacecraft charge-neutral. In a thruster design consisting of multiple membrane ionizers in a thin laminate structure with a peripheral accelerator grid, the direction of thrust could then be controlled (without need for moving parts in the thruster) by regulating the supply of gas to specific ionizer.

This work was done by Frank T. Hartley and James B. Stephens of Caltech for **NASA's Jet Propulsion Laboratory**. *Further information is contained in a TSP (see page 1). NPO-21059*

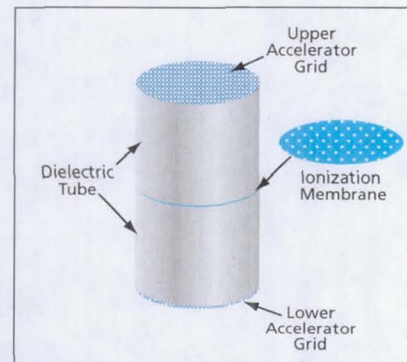# Miniature Bipolar Electrostatic Ion Thruster

All of the propellant molecules would be ionized.

NASA's Jet Propulsion Laboratory, Pasadena, California

The figure presents a concept of a bipolar miniature electrostatic ion thruster for maneuvering a small spacecraft. The ionization device in the proposed thruster would be a 0.1-micron-thick dielectric membrane with metal electrodes on both sides. Small conical holes would be micromachined through the membrane and electrodes. An electric potential of the order of a volt applied between the membrane electrodes would give rise to an electric field of the order of several megavolts per meter in the submicron gap between the electrodes. An electric field of this magnitude would be sufficient to ionize all the molecules that enter the holes.

In a thruster based on this concept, one or more propellant gases would be introduced into such a membrane ionizer. Unlike in larger prior ion thrusters, all of the propellant molecules would be ionized. This thruster would be capable of bipolar operation. There would be two accelerator grids — one located forward and one located aft of the membrane ionizer. In one mode of operation, which one could denote the forward mode, positive ions leaving the ionizer on the backside would be accelerated to high momentum by an electric field between the ionizer and an accelerator grid. Electrons leaving the ionizer on the front side would be ejected into free space by a smaller accelerating field. The equality of the ion and electron currents would eliminate the need for an additional electron- or ion-emitting device to keep the spacecraft charge-neutral. In another mode of operation, which could denote the reverse mode, the polarities of the voltages applied to the accelerator grids and to the electrodes of the membrane ionizer would be the reverse of those of the forward mode. The reversal of electric fields would cause the ions and electrons to be ejected in the reverse of their forward-mode directions, thereby giving rise to thrust in the direction opposite that of the forward mode.

A **Proposed Miniature Bipolar Electrostatic Ion Thruster** would include an ionization membrane. An electric potential between the membrane electrodes would produce an electric field that would generate ions.

Holographic Plossl Retroreflectors

Lightweight, inexpensive holographic optical elements would be used in place of lenses.

*Goddard Space Flight Center, Greenbelt, Maryland*

Holographic retroreflectors that function equivalently to Plossl eyepieces have been developed and used in free-space optical communication systems that utilize laser beams. Plossl eyepieces are well known among telescope designers. They have been adopted for use as retroreflectors and as focusing elements (for reception) and collimating elements (for transmission) in optical communication systems. A retroreflector that incorporates a Plossl eyepiece is termed a cat's-eye retroreflector (see figure).

Plossl eyepieces have external pupils and are telecentric. Their telecentricity is what makes them useful as retroreflectors. A Plossl eyepiece is necessarily somewhat complex and expensive because it contains lenses that must be optically corrected to enable operation over a large field of view and a range of visible wavelengths.

In a free-space optical communication system, there is no need for lenses that function over a range of wavelengths because only one wavelength — the laser wavelength — is used to transmit information. A holographic optical element can readily be designed to perform equivalently to a corrected lens assembly at a single wavelength. If the Plossl eyepiece in a cat's-eye retroreflector were replaced with a holographic optical element, the resulting optical assembly would be simpler and considerably lighter in weight. In addition, in mass production, such holographic optical elements would cost much less than do the corresponding lenses.
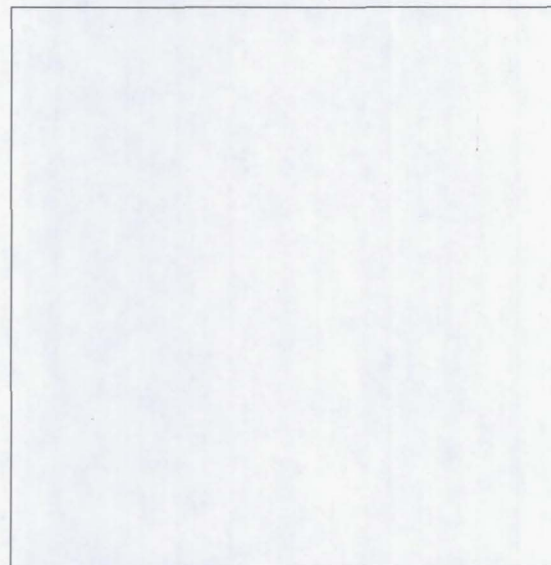
A **Cat's-Eye Retroreflector** can contain a Plossl eyepiece or, as proposed, could contain a holographic optical element that would act like a Plossl eyepiece at a single wavelength. The holographic element would, in effect, act as an ideal thin lens.

Miniature Electrostatic Ion Thruster With Magnet

NASA's Jet Propulsion Laboratory, Pasadena, California

A miniature electrostatic ion thruster is proposed that, with one exception, would be based on the same principles as those of the device described in the previous article, "Miniature Bipolar Electrostatic Ion Thruster" (NPO-21057). The exceptional feature of this thruster would be that, in addition to using electric fields for linear acceleration of ions and electrons, it would use a magnetic field to rotationally accelerate slow electrons into the ion stream to neutralize the ions.

Using Apex To Construct CPM-GOMS Models

Models of human/computer interaction are generated automatically from descriptions of tasks.

Ames Research Center, Moffett Field, California

A process for automatically generating computational models of human/computer interactions as well as graphical and textual representations of the models has been built on the conceptual foundation of a method known in the art as CPM-GOMS. This method is so named because it combines (1) the task decomposition of analysis according to an underlying method known in the art as the goals, operators, methods, and selection (GOMS) method with (2) a model of human resource usage at the level of cognitive, perceptual, and motor (CPM) operations. CPM-GOMS models have made accurate predictions about behaviors of skilled computer users in routine tasks, but heretofore, such models have been generated in a tedious, error-prone manual process.

In the present process, CPM-GOMS models are generated automatically from a hierarchical task decomposition expressed by use of a computer program, known as Apex, designed previously to be used to model human behavior in complex, dynamic tasks. An inherent capability of Apex for scheduling of resources automates the difficult task of interleaving the cognitive, perceptual, and motor resources that underlie common task operators (e.g., move and click mouse). The user interface of Apex automatically generates Program Evaluation Review Technique (PERT) charts, which enable modelers to visualize the complex parallel behavior represented by a model. Because interleaving and the generation of displays to aid visualization are automated, it is now feasible to construct arbitrarily long sequences of behaviors.

The process was tested by using Apex to create a CPM-GOMS model of a relatively simple human/computer-interaction task and comparing the time predictions of the model and measurements of the times taken by human users in performing the various steps of the task. The task was to withdraw $80 in cash from an automated teller machine (ATM). For the test, a Visual Basic mockup of an ATM was created, with a provision for input from (and measure-ment of the performance of) the user via a mouse.

The times predicted by the automatically generated model turned out to approximate the measured times fairly well (see figure). While these results are promising, there is need for further development of the process. Moreover, it will also be necessary to test other, more complex models: The actions required of the user in the ATM task are too sequential to involve substantial parallelism and interleaving and, hence, do not serve as an adequate test of the unique strength of CPM-GOMS models to accommodate parallelism and interleaving.

This work was done by Bonnie John of Carnegie Mellon University and Alonso Vera, Michael Matessa, Michael Freed, and Roger Remington of **Ames Research Center**. *Further information is contained in a TSP (see page 1).*

Inquiries concerning rights for the commercial use of this invention should be addressed to the Technology Partnerships Division, Ames Research Center, (650) 604-2954. Refer to ARC-15072-1.
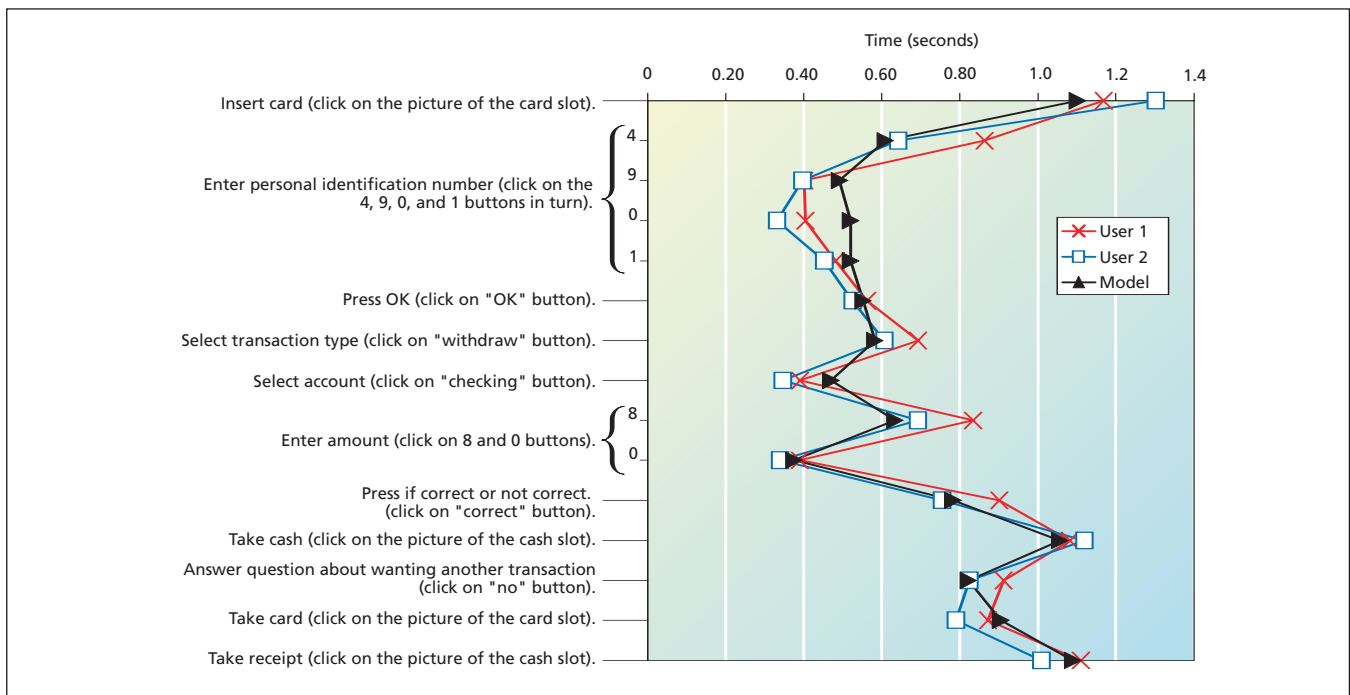
Times Taken in the Various Steps of a simulated withdrawal of cash from an ATM were predicted by an automatically generated model and measured in sequences of 10 error-free trials of two users who had practiced the task.

Sequence Detection for PPM Optical Communication With ISI

Inter-symbol interference could be reduced.

NASA's Jet Propulsion Laboratory, Pasadena, California

A method of sequence detection has been proposed to mitigate the effects of inter-slot interference and inter-symbol interference (both denoted "ISI") in the reception of M-ary pulse-position modulation (PPM) optical signals. The method would make it possible to reduce the error rate for a given slot duration, to use a shorter slot duration (and, hence, to communicate at a higher rate) without exceeding a given error rate, or to use a lower-bandwidth (and, hence, less-expensive) receiver to receive a signal of a given slot width without exceeding a given error rate.

In M-ary PPM, a symbol period is divided into M time slots, each of duration T_s, and a symbol consists of a binary sequence — ones and zeros — represented by pulses or the absence of pulses, respectively, in the time slots. At the transmitter, the bit stream is used to modulate a laser, the output of which is constant (either full power or zero power, representing 1 or 0, respectively) during each time slot. However, the signal becomes attenuated (signal photons are lost) in propagation from the transmitter to the receiver and noise enters at the receiver, complicating the problem of determining the timing of the symbol periods and slots and identifying the symbols.

The photodetector in a PPM receiver produces a pulse in response to each incident photon, so that, in effect, the receiver counts arriving signal photons. Because the duration of each pulse is finite, the response of the detector during a given time slot can include or consist of one or more tails of pulses from photons belonging to the preceding time slot (see figure). As a result, depending on the bit-to-symbol mapping of the PPM code in use, the receiver could interpret the current received symbol as other than the intended symbol. ISI is the tendency toward erroneous interpretation of this kind. The severity of ISI increases as T_s decreases. Hence, the pulse duration imposes a lower limit on the range of useable T_s values.

The present method of reducing ISI involves mathematical modeling of ISI, a novel bit-to-symbol mapping (that is, a novel PPM code), and an iterative demodulation-and-decoding scheme. The method can be implemented in a re-

This **Example of a Detector Output** was simulated, using part of a sinc function with a main-lobe width of $T_s/2$ as a model of the detector response to a single photon. ISI occurs because a significant fraction of the response to a photon arriving in a given time slot occurs in the following time slot.

ceiver of relatively low complexity.

In the mathematical model, photons are assumed to arrive at randomly distributed instants during each time slot. The number of photons arriving during a time slot is assumed to be Poisson-distributed, with mean n_b in a noise-only ("0") slot or mean $n_s(1 - \beta/2) + n_b$ during a signal-plus-noise ("1") slot, where β is the average detector-output energy that appears in the adjacent time slots. The fraction β depends on the shape of the detector output pulse. The method includes dividing each T_s into a number (typically, 64) of sampling periods and summing the digitized detector-output samples from these periods to estimate the integral of the detector-output waveform. The sums thus computed are used, in conjunction with the mathematical model, to form likelihoods for the iterative demodulation-and-decoding scheme.

The novel bit-symbol mapping, denoted anti-Gray, stands in contrast with two prior mappings, denoted natural and Gray, respectively. In a natural mapping, an input a (where a is an integer between 0 and $M - 1$) is mapped to a pulse in position a. In a Gray mapping, pairs of PPM symbols characterized by pulses in adjacent slots are mapped to input pairs with minimal Hamming distance (1). In an anti-Gray mapping, pairs of PPM symbols with pulses in adjacent slots are mapped to input pairs with maximal Hamming distance [$\log_2(M)$ or $\log_2(M) - 1$]. By means of computational simulations, it has been shown that an anti-Gray mapping reduces bit and word error rates, relative to those of a natural mapping, by amounts that correspond to a 0.25 dB increase in signal strength.

Algorithm for Rapid Searching Among Star-Catalog Entries

Recursive algorithm utilizes precompiled search structure of spherical coverings.

*NASA's Jet Propulsion Laboratory, Pasadena, California*

An algorithm searches a star catalog to identify guide stars within the field of view of a telescope or camera. The algorithm is fast: the number of computations needed to perform the search is approximately proportional to the logarithm of the number of stars in the catalog.

The algorithm requires the prior organization of the star catalog into a hierarchy utilizing independent spherical coverings (see figure), such that each successively higher level contains fewer elements. In the lowest and most numerous level of the hierarchy, the elements are individual stars in the star catalog. The next higher level contains a spherical covering (a constellation of n points on a sphere that minimizes the maximum distance of any point on the sphere from the closest one of the n points), the next higher level contains a smaller spherical covering, and so forth, ending at the highest level, which contains one element representing the point of entry into the search structure.

With necessary exceptions at the lowest and highest levels, each element at each level is labeled in terms of the element to which it is linked in the next higher level and the first element to which it is linked in the next lower level. Each element is also labeled in terms of (1) its coordinates on the celestial sphere and (2) the largest angular distance to any element in any lower level in the hierarchy. The elements at all levels of the hierarchy are numbered on a single list, such that the elements of each constellation at each level are numbered consecutively. The algorithm is recursive.

The input required to start the algorithm comprises the coordinates of a point on the celestial sphere. Attention is then focused on individual elements of the hierarchy, starting from the topmost one, as follows: The angle between the input point and the element under consideration is calculated. If the calculated angle is larger than the sum of (1) the predetermined angle to the most distant element plus (2) the half field of view of the telescope, then no stars will be within the field of view and this recursive part of the algorithm is terminated. If the calculated angle is smaller than the aforesaid sum, then the focus of attention is shifted to the elements in the next lower level of the hierarchy, in numerical order. The foregoing operations are repeated until either the algorithm is terminated or the focus of attention reaches an element at the lowest level (a star-catalog entry). In the latter case, the star is identified as being in the field of view.
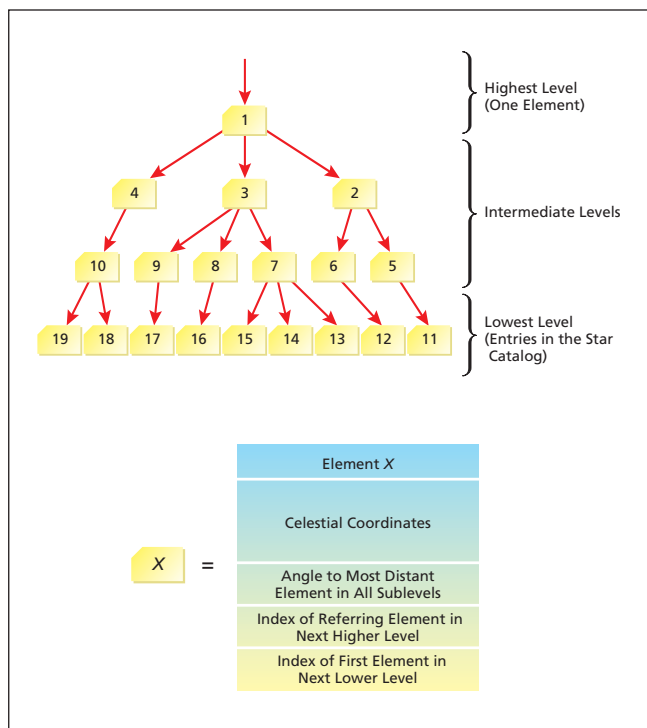
A **Hierarchy of Sequentially Numbered Elements** is created from entries in a star catalog. In this example, the hierarchy is based on nine stars and includes a total of four levels.

This work was done by Carl Christian Liebe of Caltech for **NASA's Jet Propulsion Laboratory**. *Further information is contained in a TSP (see page 1).*

The software used in this innovation is available for commercial licensing. Please contact Karina Edmonds of the California Institute of Technology at (818) 393-2827. Refer to NPO-40823.

Expectation-Based Control of Noise and Chaos

NASA's Jet Propulsion Laboratory, Pasadena, California

A proposed approach to control of noise and chaos in dynamic systems would supplement conventional methods. The approach is based on fictitious forces composed of expectations governed by Fokker-Planck or Liouville equations that describe the evolution of the probability densities of the controlled parameters. These forces would be utilized as feedback control forces that would suppress the undesired diffusion of the controlled parameters. Examples of dynamic systems in which the approach is expected to prove beneficial include spacecraft, electronic systems, and coupled lasers.

This work was done by Michail Zak of Caltech for **NASA's Jet Propulsion Laboratory**. *Further information is contained in a TSP (see page 1).*
NPO-41792

NASA Tech Briefs, November 2006
35

Books & Reports

Radio Heating of Lunar Soil To Release Gases

A report proposes the development of a system to collect volatile elements and compounds from Lunar soil for use in supporting habitation and processing into rocket fuel. Prior exploratory missions revealed that H_2, He, and N_2 are present in Lunar soil and there are some indications that water ice may also be present. The proposed system would include a shroud that would be placed on the Lunar surface. Inside the shroud would be a radio antenna aimed downward. The antenna would be excited at a suitably high power and at a frequency chosen to optimize the depth of penetration of radio waves into the soil. The radio waves would heat the soil, thereby releasing volatiles bound to soil particles. The escaping volatiles would be retained by the shroud and collected by condensation in a radiatively cooled vessel connected to the shroud. It has been estimated that through radio-frequency heating at a power of 10 kW for one day, it should be possible to increase the temperature of a soil volume of about 1 m^3 by about 200 °C — an amount that should suffice for harvesting a significant quantity of volatile material.

This work was done by Talso Chui and Konstantin Penanen of Caltech for **NASA's Jet Propulsion Laboratory**. *Further information is contained in a TSP (see page 1).* NPO-43313

Using Electrostriction To Manipulate Ullage in Microgravity

A report proposes to use electrostriction to manipulate the ullage in a tank containing a dielectric liquid in a microgravitational environment. In the original intended application, the liquid would be a spacecraft propellant and the goal would be to force the ullage (comprising bubbles of noncondensible gas) to coalesce at one end of the tank, to enable use of one of the established means of (1) measuring the position of the gas/liquid interface and (2) inferring the quantity of liquid from the measurement. Electrically insulated wires would be installed in the tank, shaped and positioned so that application of a suitably high potential (e.g., 1 kV) between adjacent wires in successive pairs would give rise to a sufficient electric field gradient along

the tank. The resulting electrostriction in the liquid would give rise to a pressure gradient that would force the ullage toward the low-electric-field-magnitude end of the tank. The feasibility of this proposal was demonstrated in an experiment in a tank containing liquid helium aboard an airplane flying a low-gravity arc. The ullage-segregating electrostrictive effect is expected to be considerably greater in other liquids.

This work was done by Talso Chui and Donald Strayer of Caltech for **NASA's Jet Propulsion Laboratory**. *Further information is contained in a TSP (see page 1).* NPO-43041

Equations for Scoring Rules When Data Are Missing

A document presents equations for scoring rules in a diagnostic and/or prognostic artificial-intelligence software system of the rule-based inference-engine type. The equations define a set of metrics that characterize the evaluation of a rule when data required for the antecedence clause(s) of the rule are missing. The metrics include a primary measure denoted the rule completeness metric (RCM) plus a number of subsidiary measures that contribute to the RCM. The RCM is derived from an analysis of a rule with respect to its truth and a measure of the completeness of its input data. The derivation is such that the truth value of an antecedent is independent of the measure of its completeness. The RCM can be used to compare the degree of completeness of two or more rules with respect to a given set of data. Hence, the RCM can be used as a guide to choosing among rules during the rule-selection phase of operation of the artificial-intelligence system.

This work was done by Mark James of Caltech for **NASA's Jet Propulsion Laboratory**. *Further information is contained in a TSP (see page 1).*

The software used in this innovation is available for commercial licensing. Please contact Karina Edmonds of the California Institute of Technology at (818) 393-2827. Refer to NPO-42717.

Insulating Material for Next-Generation Spacecraft

A report discusses the development of a flexible thermal-insulation material for cryogenic tanks in next-generation space-

craft. This material is denoted Advanced Reusable All-temperature Multimode Insulation System (ARAMIS). The report begins by describing the need for ARAMIS and the technological challenges of developing a single material that is useable throughout the temperature range from storage of liquid hydrogen (20 K) to atmospheric-reentry heating (>2,000 K), has the requisite low thermal conductivity, resists condensation of moisture without need for a gas purge, and withstands reentry heating for a 400-mission lifetime. The report then discusses laboratory apparatuses for testing materials that have been and will be considered as candidates for the development of ARAMIS.
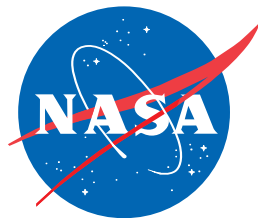
This work was done by Susan White, Sylvia Johnson, Louis Salerno, Peter Kittel, and Pat Roach of **Ames Research Center** *and Ben Helvensteijn and Ali Kashani of Atlas Scientific. Further information is contained in a TSP (see page 1).*

Inquiries concerning rights for the commercial use of this invention should be addressed to the Ames Technology Partnerships Division at (650) 604-2954. Refer to ARC-14727-1.

Pseudorandom Switching for Adding Radar to the AFF Sensor

A document describes the proposed addition of a radar function to the Autonomous Formation Flying Sensor, making possible coarse relative-position control to prevent collisions in the event of failure of one of the spacecraft. According to the proposal, in addition to tracking GPS-like one-way ranging signals transmitted by the other normally functioning spacecraft, each spacecraft could simultaneously track the reflection of its own ranging signal from a disabled, non-transmitting spacecraft. From the round-trip travel time, the approximate distance to the disabled spacecraft could be estimated. To prevent jamming of the receiver by the transmitter on the same spacecraft, the receiver would be switched off during transmission.

This work was done by Jeffrey Tien, George Purcell, and Lawrence Young of Caltech for **NASA's Jet Propulsion Laboratory**. *Further information is contained in a TSP (see page 1). NPO-40417*

National Aeronautics and
Space Administration